THESIS

(1)

SEARCH FOR THE PHOTO-INDUCED PHASE TRANSITION IN ORGANIC SOLIDS

有機固体における光誘起相転移の探索

Shin-ya KOSHIHARA

腰　原　伸　也

SUBMITTED TO

DEPARTMENT OF PHYSICS

FACULTY OF SCIENCE

THE UNIVERSITY OF TOKYO

MAY, 1991

THESIS

(1)

SEARCH FOR THE PHOTO-INDUCED PHASE TRANSITION IN ORGANIC SOLIDS

有機固体における光誘起相転移の探索

Shin-ya KOSHIHARA

腰　原　伸　也

SUBMITTED TO

DEPARTMENT OF PHYSICS

FACULTY OF SCIENCE

THE UNIVERSITY OF TOKYO

MAY, 1991

ACKNOWLEDGMENT

I would like to express my sincerest gratitude to Professor Yoshinori Tokura for his helpful suggestions, guidance and encouragement throughout the course of the present work. I am indebted to Prof.G.Saito and Dr.K.Takeda for preparation of samples and enlightening discussion. I am also indebted to Dr.A.Kobayashi for her help in X-ray diffraction measurements, and to Prof.S.Uchida for the use of X-ray diffractometer. I am grateful to Prof.T.Koda, Prof.T.Mitani, Prof.H.Tanaka, Drs.Y.Iwasa, K.Ishikawa, T. Kanetake and H.Okamoto, and Messrs.H.Moritomo, T.Arima and H.Hasegawa for valuable discussion. I also thank all the members of the research groups under Prof.Y.Tokura, Prof.T.Koda and Prof.G.Saito. This work was supported in part by a Grant-In-Aid from the Ministry of Education, Science and Culture, Japan, and also by International Joint Research Project from the NEDO.

CONTENT

CHAPTER IV

Reversible and Irreversible Thermochromic Phase Transitions in Single Crystals of Polydiacetylenes Substituted with Alkyl-urethanes

CHAPTER V

Bi-directional Photo-switching between the Two Phases in Single Crystals of Polydiacetylenes

CHAPTER VI

CHAPTER I

General Introduction

Recently, extensive studies have been made on the structural change by optical pumping in the fields of photochemistry and solid-state physics. Those studies have been mainly concerned with microscopic reaction confined in small molecules or local structure change in crystals. Photo-induced cis-trans isomerization of azobenzene (see Fig.I-1(a)), optically induced defect state in amorphous materials (fatigued photo-luminescence center) (Fig.I-1(b)) [I-1] and self-trapped exciton in alkaline-halide (Fig.I-1(c)) [I-2] are typical examples of such a local structure change by photo-excitation. By contrast, the purpose of this study is to explore some collective channels between the photo-induced local structure changes in solids and to search for new molecular systems in which photo-irradiation can induce the electronic and lattice structure changes over macroscopic size with extremely high efficiency. In the following chapters, we will report experimental evidences indicating that the photo-injected local excitation can become the trigger of the phase transition via some cooperative interaction in several organic crystals with one-dimensional electronic structures.

In this thesis, photo-induced effects have been studied in prototypical three compounds with one-dimensional electronic structures; (1)tetrathiafulvalene(TTF)-chloranil(CA), (2)potassium(K)-tetracyanoquinodimethane (TCNQ), and (3)polydiacetylenes (PDAs) substituted with alkyl-urethane side-groups. In the following, we make a brief summary on characters of these compounds. The

(a) Photo-isomerization

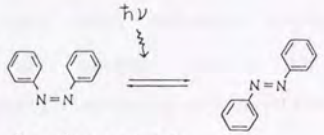

Azobenzene

(b)Microscopic Model of the Fatigued Luminescence Center

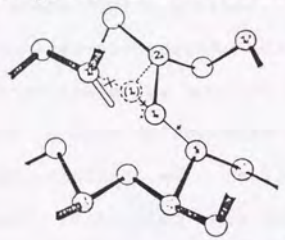

---- As atom

---- S atom

(c) Model of Self-trapped Exciton in Alkaline-halide Crystal

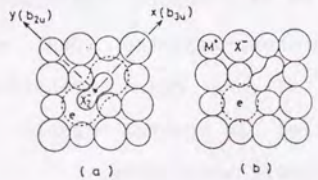

Figure I-1 : Examples of photo-induced local structure changes. (a) Cis-trans isomerization in azobenzene, (b) Defect state (fatigued photo-luminescence center) in amorphous materials ($a\text{-}As_2S_3$). (ref.I-1), and (c) self-trapped exciton in alkaline-halide (ref.I-2).

detailed discussion for respective systems will be given in respective chapters II (TTF-CA), III (K-TCNQ), IV (PDA) and V (PDA).

(1) TTF-CA is one of the mixed stack type charge-transfer compounds and composed of one dimensional chains of donor (D:TTF) and acceptor (A:CA) (see Fig.I-2)[I-3]. Single crystal of this compound undergoes the first order phase transition accompanying the changes in ionicity of constituent molecule ($:D^+ A^-$) [I-4,5] and dimeric lattice distortion (T_c=81K, hysteresis width 2deg.) [I-6]. The degree of ionicity, , is relatively high (ca. 0.7) and lattice is dimerized in the low-temperature phase, whereas the value of is low (ca. 0.3) and dimeric distortion disappears in the high-temperature phase. The high-temperature and low-temperature phases are called neutral (N) phase, and ionic (I) one, respectively. Figure I-3 schematically shows the electronic structure change upon the neutral-ionic (N-I) phase transition. Below T_c, one of the electrons in the highest occupied molecular orbital (HOMO) of the donor moves to the lowest unoccupied molecular orbital (LUMO) of the acceptor. The N-I transition can be sensitively probed by reflectance spectra in IR and VIS-UV regions as shown in Fig.I-4 [I-5]. In the temperature region around T_c, large changes in dielectric constants [I-7,8], conductivity and ESR[I-9] signal have been also reported. In chapter II, photo-induced absorption (PA) spectra in TTF-CA crystal are presented, and the possibility of the photo-induced N-I transition is discussed.

(2) K-TCNQ crystal is composed of segregated stacks of TCNQ and K as shown in Fig.I-5[I-10,11], and a complete

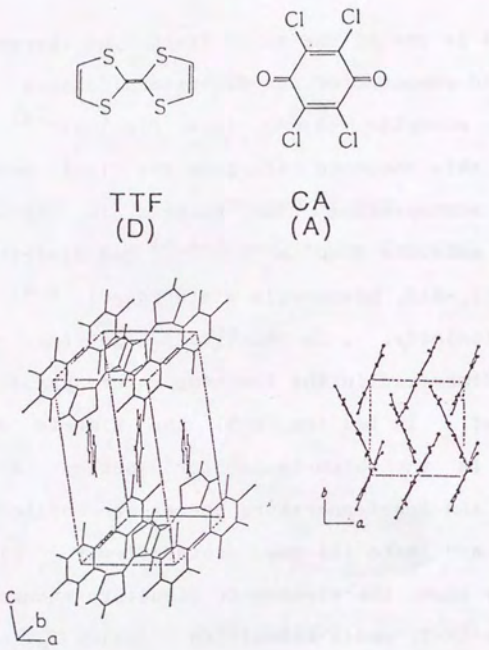

Figure I-2 : Structure of TTF-CA single crystal at R.T. (ref. I-3).

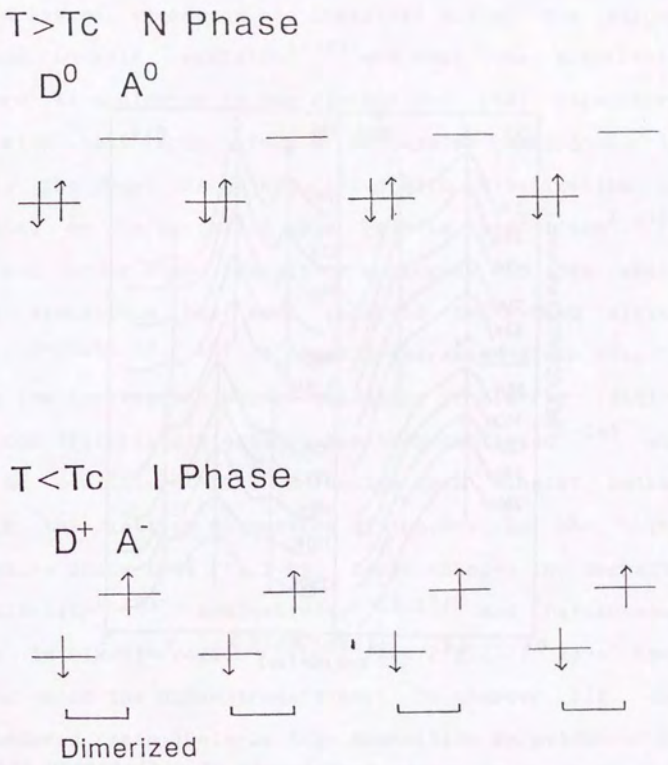

Figure I-3 : Schematics for the electronic structures of TTF-CA in the high temperature (N:neutral) and low temperature (I:ionic) phases. In the low temperature phase, occurrence of dimeric lattice distortion was confirmed by measurements of X-ray diffraction[I-6].

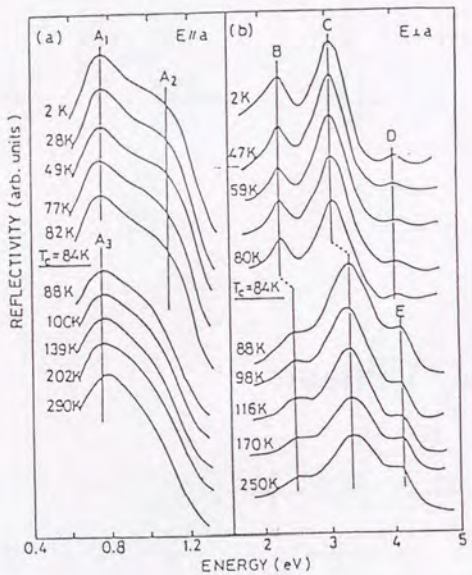

Figure I-4 : Temperature dependences of reflectance spectra for the charge-transfer excitation bands (a) and of the intra-molecular excitation bands (b) across the neutral-to-ionic phase-transition temperature (T_c=84K, ref.I-5).

charge transfer between TCNQ and K occurs (K^+ $TCNQ^-$: =1). In this system, electrons are localized due to the strong coulombic on-site repulsion[I-12] and thus the electronic structure is analogous to one dimensional (1D) Heisenberg chain with half spin. Such a 1D system undergoes, in general, the phase change associated with dimerization of spin-site, or the so-called spin Peierls transition[I-11]. The first order phase transition analogous to the spin-Peierls transition has been reported in K-TCNQ single crystal [I-10,11,13 - 16] (T_c=395K hysteresis width 5deg.). In the low-temperature phase, existence of dimeric lattice distortion (Peierls distortion) has been confirmed[I-14] and spins on constituent $TCNQ^-$ molecules form singlet pairs, although the lattice distortion disappears in the high-temperature phase (see Fig.I-6). Large changes in magnetic susceptibility[I-13], conductivity[I-11,17] and reflectance spectra in IR-VIS region[I-15,16] (see Fig.I-7) have been observed upon the phase transition. In chapter III, the photo-induced (spin-)Peierls like transition is evidenced by spectroscopic method.

(3) Polydiacetylens (PDAs: $\{CR\text{-}C{\equiv}C\text{-}CR'\}_x$, R and R' represent side groups)) are well known conjugated polymer and undergoes the phase transition accompanying drastic color change by various stimulations [I-18]. Fig.I-8 shows the thermally induced phase transition observed for ETCD ($R{=}R'{=}(CH_2)_4OCONHCH_2CH_3$) single crystals [I-19]. Generally, there are two distinct phases, blue colored low-temperature phase and red colored high-temperature one, which will be here referred as the A and B phases, respectively. The A-B transition in ETCD is thermally reversible accompanying large hysteresis width (ca. 60deg.) [I-19]. This novel

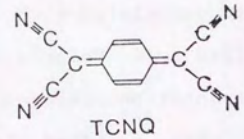

TCNQ

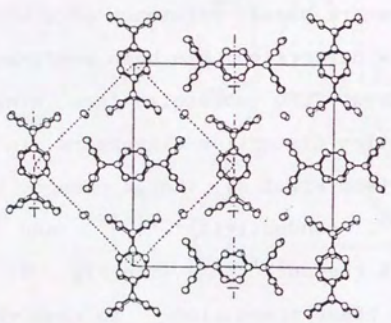

Projection along the a axis onto (100) plane

Figure I-5 : Structure of K-TCNQ single crystal in high and low temperature phases. Solid, and broken lines indicate the unit cells in low, and high temperature phases, respectively (ref.I-10 and 11).

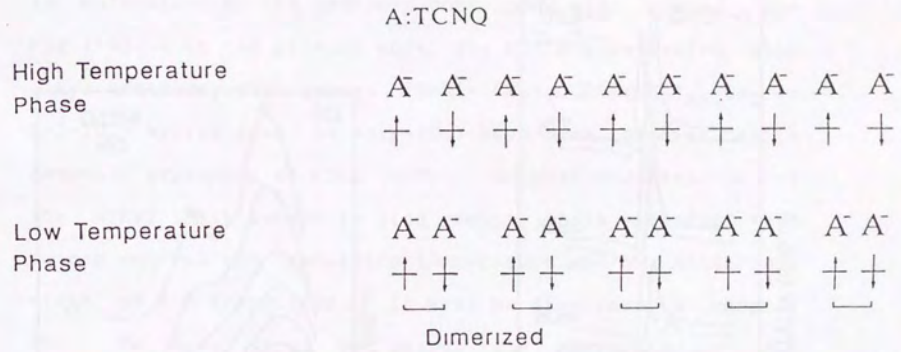

Figure I-6 : Schematics of electronic structure of K-TCNQ crystal in the high and low temperature phases.

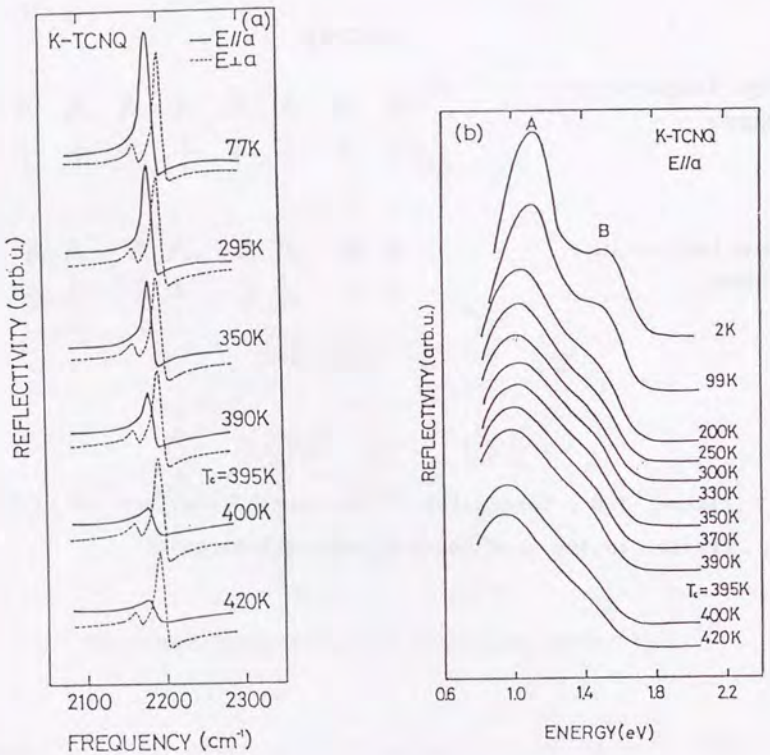

Figure I-7 : Temperature dependence of reflectance spectra in energy regions of C=N stretching vibrational mode (a) and charge-transfer excitation (b).

character of the A-B transition in ETCD has been discussed in the relation with the characteristic lattice structure of this compound, i.e. the planarity of carbon backbone which is maintained by the hydrogen bond among side groups (see Fig.I-9). In the present work, the PDA's substituted with alkyl-urethane side groups (R=R'=$(CH_2)_4OCONH(CH_2)_{n-1}CH_3$: n=1-10, abbreviated as poly-4Un) have been studied as a natural expansion of ETCD (n=2). By this modification of the alkyl chain length in side groups, it is expected that we can control the transition temperature and/or hysteresis width of A-B transition. It will be discussed in chapter IV. We have tried to detect the photo-induced A-B transition extensively on this new family of PDAs and have obtained definite experimental evidences for the bi-directional (A-to-B and B-to-A) phase switching by photo-excitation. Details of the photo-induced phase transition in single crystals of poly-4U3 (n=3) and relating new features are to be described in chapter V.

In this thesis, we have investigated the photo-induced effects in the above mentioned three systems. All the three systems similarly show the first order phase transition. When crystals are kept at temperature around T_c, photo-induced phase transition is expected to occur easily with weak excitation intensity due to the decreases in difference between energy levels in the high- and low-temperature phases.

The first order phase transition is common future of these systems, but the width of hysteresis in the PDA is quite different from the other (TTF-CA and K-TCNQ) cases. Such a difference in hysteresis width will cause a variety

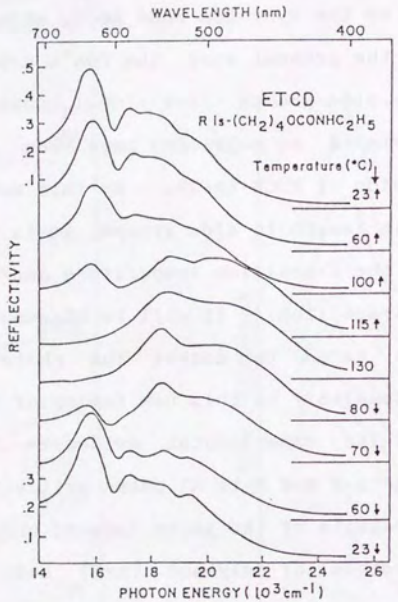

Figure I-8 : Reflectance spectra of ETCD as a function of temperature (ref. I-19).

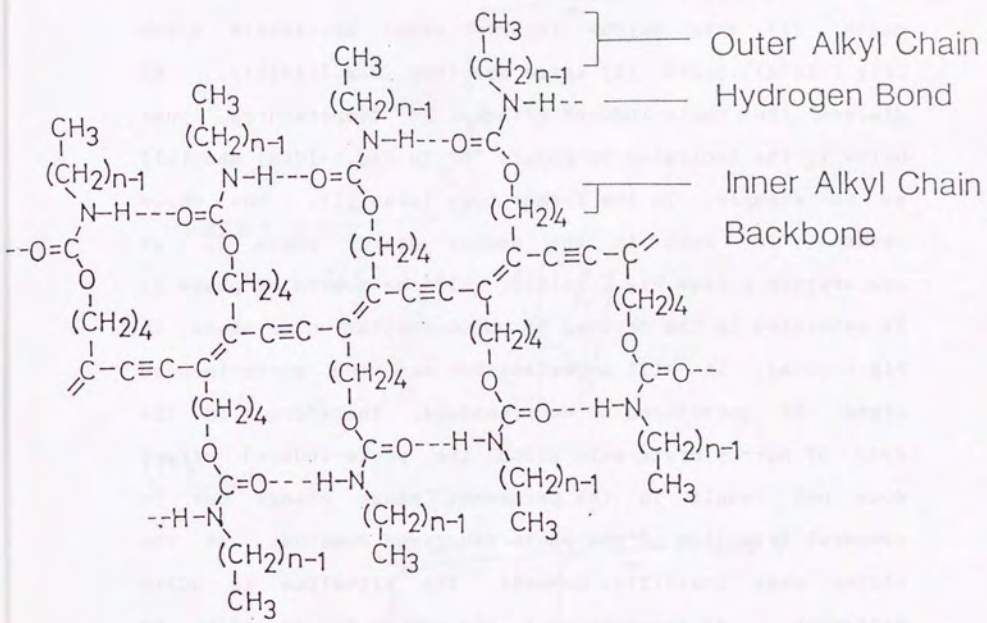

Figure I-9 : Structure of poly-4Un. Dashed lines show chains of hydrogen bonds between side-groups running parallel to the polymer backbones.

of the transient behaviors of photo-induced effect as discussed below. Here, let us consider the two exaggerated cases; (1) very narrow (nearly zero) hysteresis width (Fig.I-10(a)), and (2) large one (see Fig.I-10(b)). We discuss the photo-induced effects at temperatures just below T_c (as indicated by points "A" in Fig.I-10(a) and (b)) as an example. In the former case (case(1)), the whole crystal is kept in the stable state, phase I, at temperature A (see Fig.I-10(a)). If the domain of phase II is generated in the crystal by photo-excitation as shown in Fig.I-10(a), it will be metastable and the photo-induced signal is considered to be transient. Therefore, in the case of narrow hysteresis width, the photo-induced effect dose not result in the permanent phase change but in temporal injection of the photo-generated domains. In the latter case (case(2)), however, the situation is quite different. At temperature A, the system is deduced to be kept in the metastable phase (phase II) rather than the absolutely stable state (phase I) due to the large energy barrier between the two phases. Therefore the photo-induced effect may become permanent, if the domain of the phase I is generated in the relaxation process after the initial photo-excitation (see the schematic of Fig.I-10(b)). In other words, the permanent and macroscopic photo-induced phase transition can be expected in the case of large hysteresis width. In accord with this expectation, it has been found that the photo-induced domain injection occurs in TTF-CA and K-TCNQ giving rise to transient photo-induced signals, and the photo-induced phase transition in PDA. Detailed discussion will be given in the following chapters and the conclusion is described in the final chapter (VI).

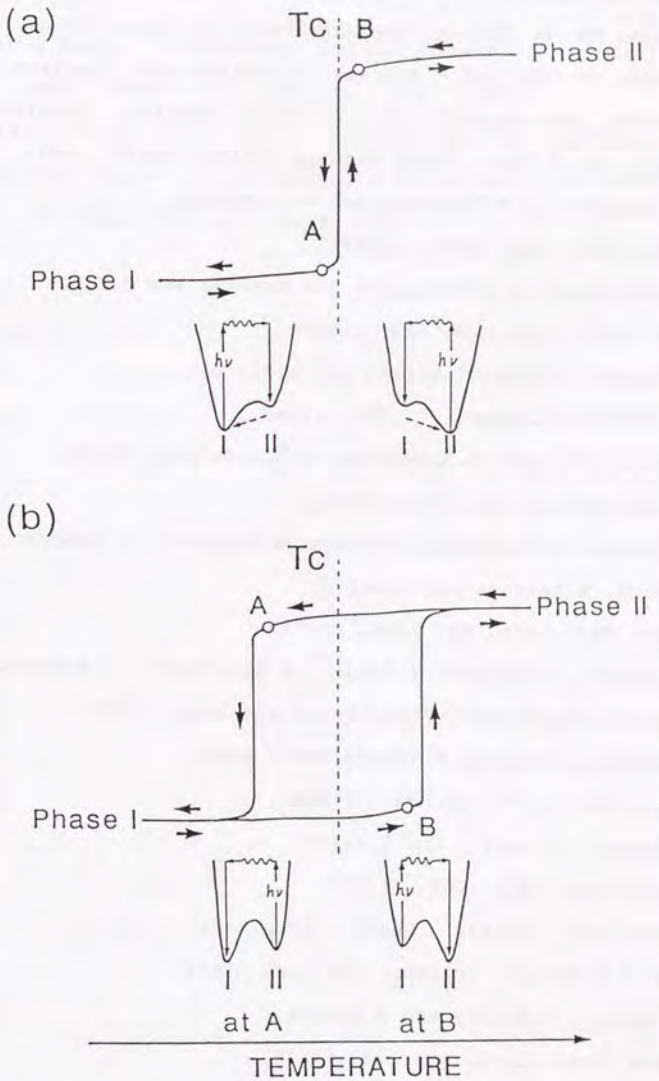

Figure I-10 : Hysteresis loops of the first order phase transition between phase I (low temperature phase) and II (high temperature phase) with (a) narrow or zero width and (b) large width. Photo-injected domain will be metastable, and stable in the cases of (a), and (b), respectively, as shown in the schematic energy level diagrams.

REFERENCES OF CHAPTER I

I-1) T.Tada, Ph. D. Thesis, The University of Tokyo (1990).

I-2) N.Itho, in 'Optical Properties of Solids and Electron-lattice Interaction', Solid State Physics, Special Issue, ed. K.Nasu, (Agne Gijutsu Center, Tokyo, 1987).

I-3) J.J.Mayerle, J.B.Torrance and J.I.Crowley, Acta Cryst. B35, 2988, (1979).

I-4) J.B.Torrance, J.E.Vanzquez, J.J.Mayerle and V.Y.Lee, Phys. Rev. Lett. 46, 253, (1981).

I-5) Y.Tokura, T.Koda, T.Mitani and G.Saito, Solid State Commun. 43, 757, (1982).

I-6) Y.Kanai, M.Tani, S.Kagoshima, Y.Tokura and T.Koda, Synth. Metals, 10, 157, (1984).

I-7) Y.Tokura, S.Koshihara, Y.Iwasa, H.Okamoto, T.Komatsu, T.Koda, N.Iwasawa and G.Saito, Phys. Rev. Lett. 63, 2405, (1988).

I-8) H.Okamoto, T.Mitani, Y.Tokura, S.Koshihara, T.Komatsu, Y.Iwasa and T.Koda, Phys. Rev.B 43, 8224, (1991).

I-9) T.Mitani, G.Saito, Y.Tokura and T.Koda, Phys. Rev. Lett. 53, 842, (1984).

I-10)M.Konno, T.Ishii and Y.Saito, Acta Cryst. B33, 763, (1977).

I-11)"Extended Linear Chain Compounds" vol.3, ed. J.S.Miller, (Plenum, New York 1983).

I-12)K.Yakusi, T.Kusaka and H.Kuroda, Chem. Phys. Lett. 68, 139, (1979).

I-13)J.G.Vegter, T.Hibma and J.Kommandeur, Chem. Phys. Lett. 3, 427, (1969).

I-14)H.Terauchi, Phys. Rev. B 17, 2446, (1978).

I-15)H.Okamoto, Ph.D.Thesis, The University of Tokyo, (1988).

I-16)H.Okamoto, Y.Tokura and T.Koda, Phys. Rev. B 36, 3858, (1987).

I-17)N.Sakai, I.Shirotani and S.Minomura, Bull. Chem. Soc. Jpn. 45, 3321, (1972).

I-18)Y.Tokura, Solid State Physics, 20, 845, (1985).

I-19)R.R.Chance, R.H.Baughman, H.Muller and C.J.Eckhardt, J. Chem. Phys. 67, 3616, (1977).

CHAPTER II

Photo-Induced Valence Instability in Organic Molecular Compound: Tetrathiafulvalene (TTF)-Chloranil (CA)

II-1 INTRODUCTION

The Tetrathiafulvalene (TTF) - Chloranil (CA) is one of the charge-transfer (CT) complexes which consists of one dimensional mixed-type stack of acceptor(A;CA) and donor(D;TTF) as shown in Fig.II-1[II-1]. The first order transition at ambient pressure (T_c=81 K) was confirmed in single crystal as mentioned in chapter I[II-2,3]. In particular, spectroscopic studies have revealed that abrupt and significant changes occur at T_c in reflection bands in VIS-UV and IR regions (Fig.II-2 and 3) [II-3,4]. Assignment of observed reflection bands is as follows: (1) In VIS-UV region, the bands B and C are attributed to intra-molecular excitations of TTF^+ molecules, and the bands D and E of TTF^0 molecules. (2) In IR region, reflection bands around 1120 and 1600 cm^{-1} are due to molecular vibration of CA with b_{1u} symmetry. These bands strongly correlate with the ionicity (ρ ; $D^{+\rho}A^{-\rho}$) of the constituent molecule [II-5]. The temperature dependence of ρ which was estimated from the frequency change of C=O stretching mode, (Fig.II-4) shows that TTF-CA single crystal undergoes the phase change from the quasi-neutral (N) to quasi-ionic (I) state when cooled below T_c ($\simeq$81K). Of course, the charged states shown in Fig.II-5 is schematic. In reality, the estimated ionicity of the molecule is fractional (ca.0.3 in the N-phase and ca.0.7 in the I-phase) due to the CT interaction ($\simeq$0.2 eV) [II-3,4] between the D and A molecules. Therefore, both of the neutral and ionic molecular

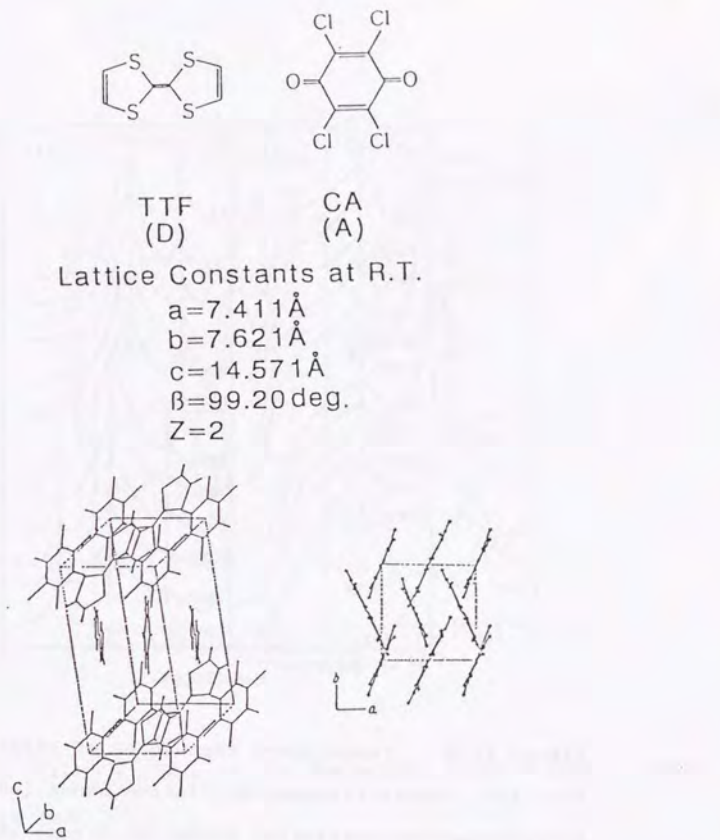

Figure II-1 : Structure and lattice parameters of TTF-CA single crystal at R.T. (ref.II-1).

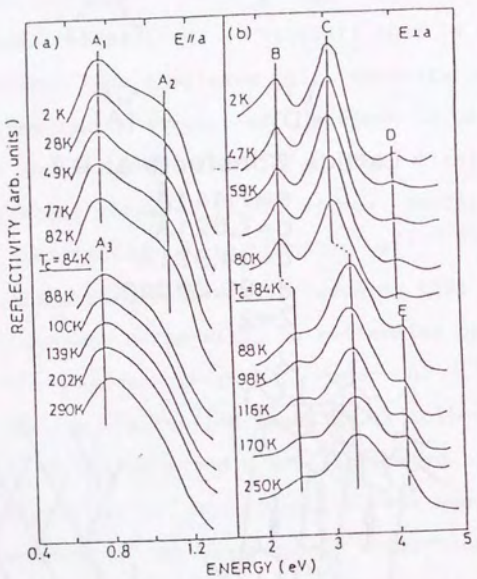

Figure II-2 : Temperature dependence of reflectance spectra for the charge-transfer excitation bands (a) and of the intra-molecular excitation bands (b) across the neutral-to-ionic phase-transition temperature T_c (ref.II-3).

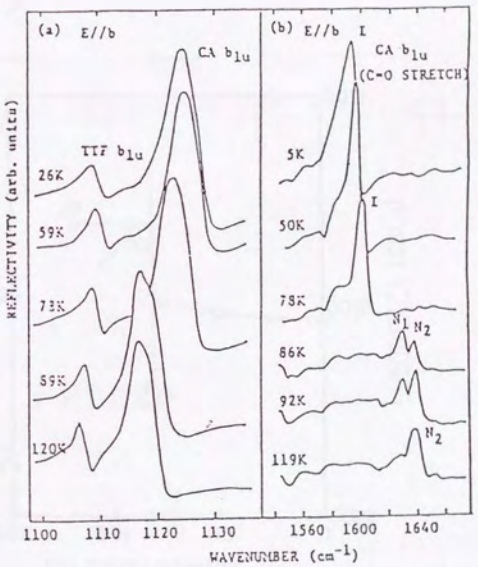

Figure II-3 : Temperature dependence of IR reflectance spectra (ref.II-4).

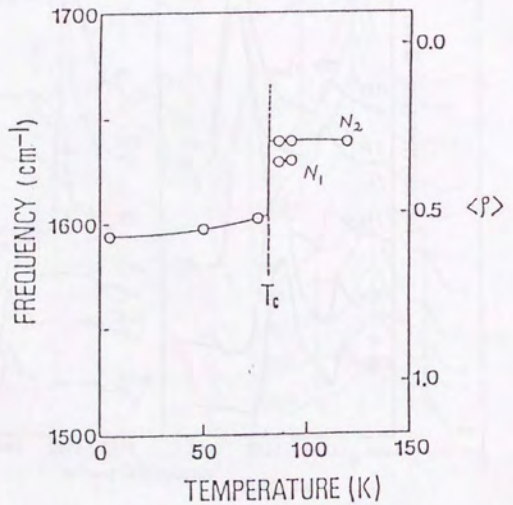

Figure II-4 : Temperature dependence of the frequency of C=O stretching vibrational mode and estimated ionicity ρ (ref.II-4).

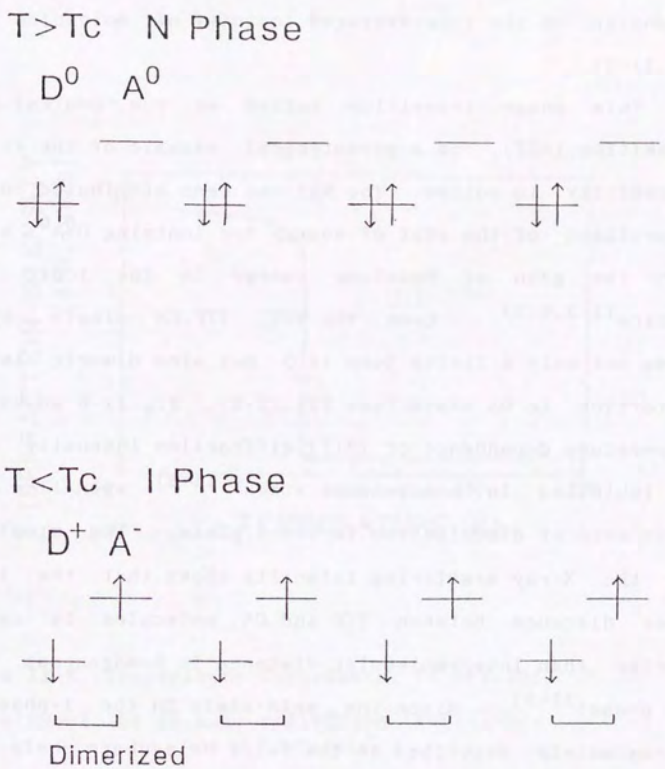

Figure II-5: Schematics for the electronic structures of TTf-CA in the high temperature (N:neutral) and low temperature (I:ionic) phases. In the low temperature phase, occurrence of dimeric lattice distortion was confirmed by measurements of X-ray diffraction[II-8].

transitions are observed simultaneously in the N or I state, but at different energies and with different intensities depending on the time-averaged ionicity of molecules (see Fig.II-2).

This phase transition, called as the neutral-ionic transition (NIT), is a prototypical example of the valence instability in solids. The NIT has been attributed to the competition of the cost of energy for ionizing D^0A^0 stacks with the gain of Madelung energy in the ionic D^+A^- lattice[II-2,6,7]. Upon the NIT, TTF-CA single crystal shows not only a finite jump in ρ but also dimeric lattice distortion in DA stack (see fig.II-5). Fig.II-6 shows the temperature dependence of $(31\bar{1})$ diffraction intensity which is inhibited in homogeneous stack [II-8] signaling that occurrence of dimerization in the I phase. The simulation for the X-ray scattering intensity shows that the intra-dimer distance between TTF and CA molecules is ca. 1% shorter than inter-molecular distance in homogeneous stack (N phase)[II-8]. Since the spin-state in the I-phase is approximately described as the S=1/2 Heisenberg chain (see Fig.II-5), the lattice transition is likely triggered by the spin-Peierls instability[II-9]. Such an electron(spin)-lattice interaction obviously plays an important role in promoting the NIT in real systems in addition to the electrostatic mechanism, as discussed by Nagaosa et.al.[II-10-12].

The electron(spin)-lattice interaction and valence instability in this system are expected to also become the origin of low energy excited states: In the I-phase, the A and B states, which show opposite direction of dimerization are energetically degenerate (Fig.II-7). Therefore,

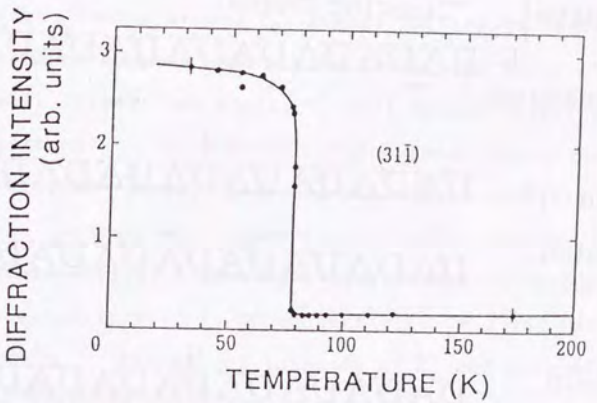

Figure II-6 :Temperature dependence, in heating run, of the intensity of the $(3,1,\bar{1})$ reflection (ref.II-8).

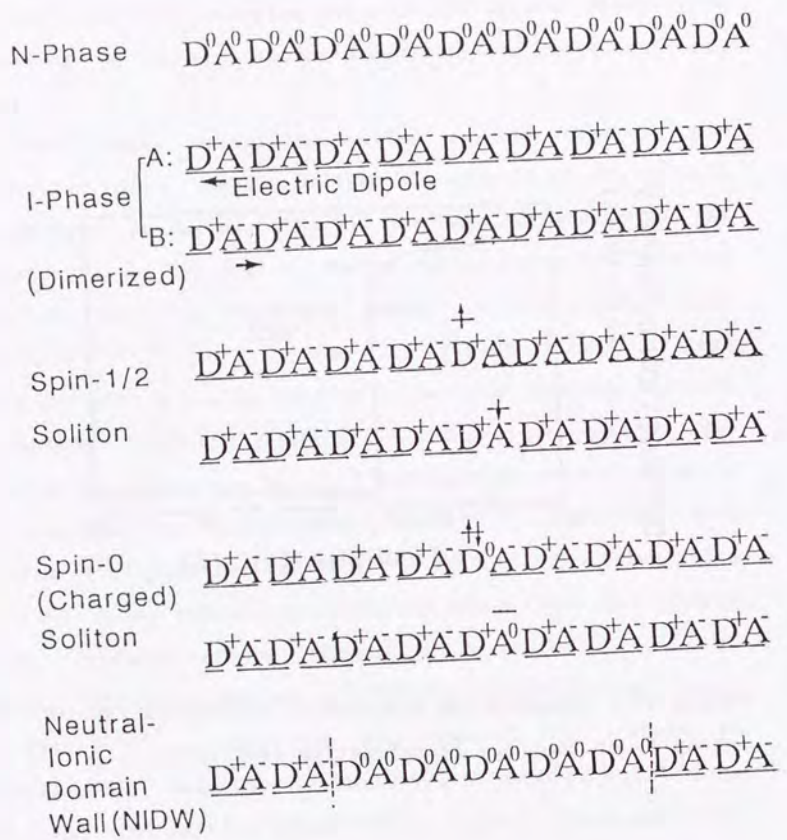

Figure II-7 :Schematics for solitons and neutral-ionic domain-walls.

existence of spin-1/2 and spin-0 solitons which connect A and B states (Fig.II-7) is expected like in the case of poly-acetylene [II-13]. In real materials, of course, the degree of ionicity (ρ) is fractional, nevertheless the present simplified model will be useful for discussion about low energy excitations in the I phase. In the temperature region around T_c, energy difference between N and I phases becomes small, and hence the neutral-ionic domain-wall (NIDW) (see Fig.II-7) will become better picture than solitons. In practice, the above mentioned low energy excited states plays an important role in novel electronic and magnetic characters of this system [II-12]. For example, Fig.II-8 shows the temperature dependences of spin-susceptibility (χ), DC conductivity (σ) and ESR line width [II-14]. The abrupt increase of χ and narrowing of ESR line width in I-phase were attributed to spin-solitons and their motion by Mitani et. al. Dramatic increases of σ and dielectric constant (see fig.II-9) [II-15] around T_c and their thermally activated type behavior may be accounted for in terms of dynamics of NIDWs. In addition, the negative-resistance effect observed in this system can be also explained as a motion of NIDW and spin-0 soliton [II-16].

In this chapter, we report the first observation that the valence instability in the DA compounds can be also caused by photo-excitation. The photo-generated CT excitations (D^0A^0) or resultant charged species (D^0 and A^0) in the ionic D^+A^- lattice locally modify the Coulombic interaction and switch off a channel of the collective electron(spin)-lattice interaction. What we have observed in this study clearly shows that those local photo-excitations serve as nuclei which evolve into the neutral molecular domains over

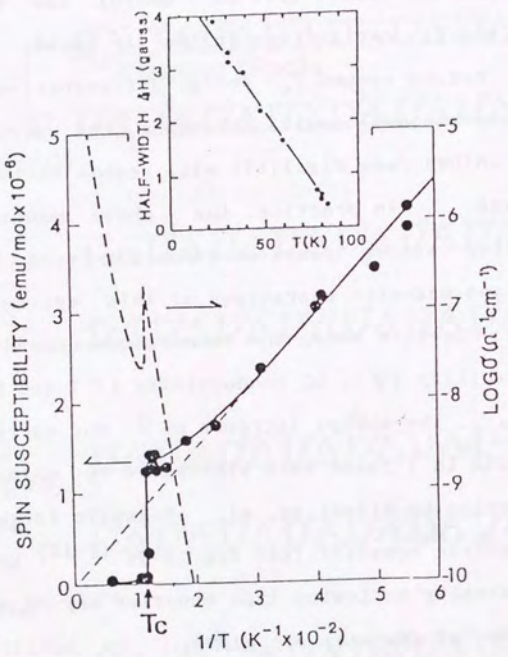

Figure II-8 :Temperature dependences of spin susceptibility, DC conductivity and ESR line width (ref. II-14).

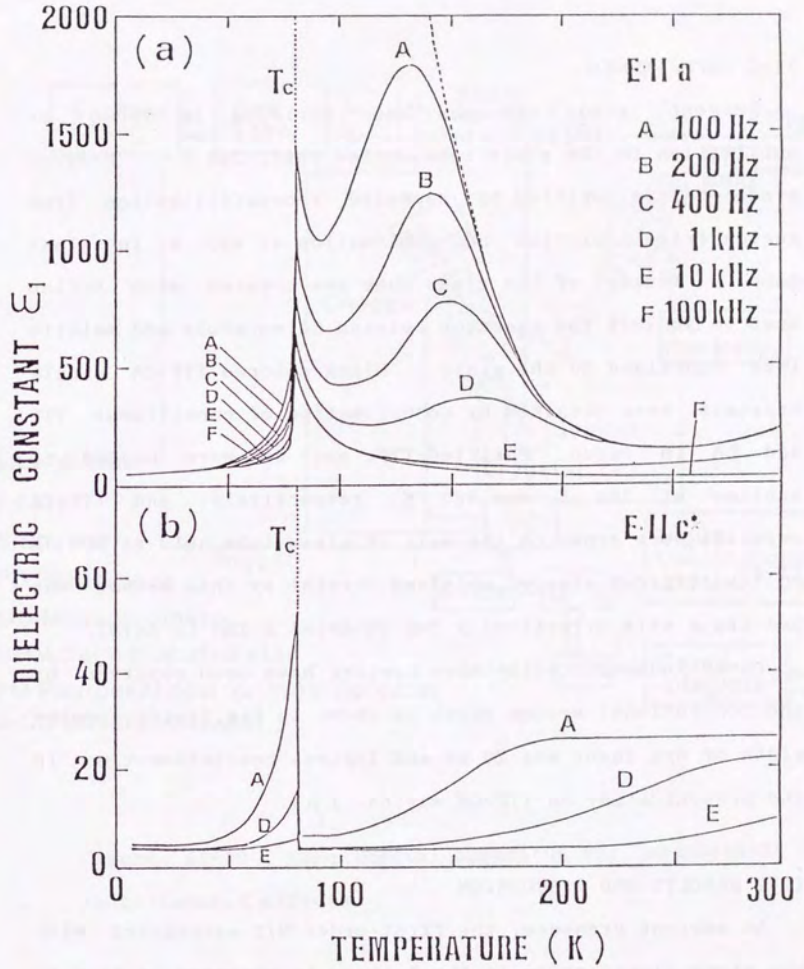

Figure II-9 :Temperature dependence of dielectric constant ε_1 at several typical frequencies with the electric field parallel to the a axis (stack axis) (a) and perpendicular to the a axis (parallel to the c* axis)(b) (ref. II-15).

a semi-macroscopic region.

II-2 EXPERIMENTAL

Reagent grade TTF has been purified in vacuo by sublimation in the glass tube heated until 345 K. Reagent grade CA is purified by repeated recrystallization from acetonitrile solution and sublimation at 430 K in glass tube. Inside of the glass tube was covered with teflon seat to inhibit the reaction between CA molecule and metalic ions contained in the glass. Black colored TTF-CA single crystals were obtained by cosublimation of constituent TTF and CA in vacuo. Purified TTF, and CA were heated to sublime at 360 K, and 380 K, respectively, and TTF-CA crystals were grown on the wall of glass tube held at 350 K II-4). Typical size of obtained crystal by this method was 3mm (in a axis direction) x 2mm (b axis) x 1mm (c axis).

Photo-induced reflectance spectra have been observed by the conventional system which is shown in Fig.II-10. Pulse width of dye laser was 20 ns and typical resolution-time in the present study on TTF-CA was ca. 1 μs.

II-2 RESULTS AND DISCUSSION

At ambient pressure, the first-order NIT associated with the stack dimerization in the I-phase is observed at 81 K in the cooling run (and at 84K in the heating run). Optical spectra for local electronic excitations have been known to be very useful to detect a change in molecular ionicity, ρ, as discussed in previous section. We discuss on the result of photo-induced effect on these molecular excitation spectra. In Fig.II-11(b) are plotted photo-reflectance (PR)

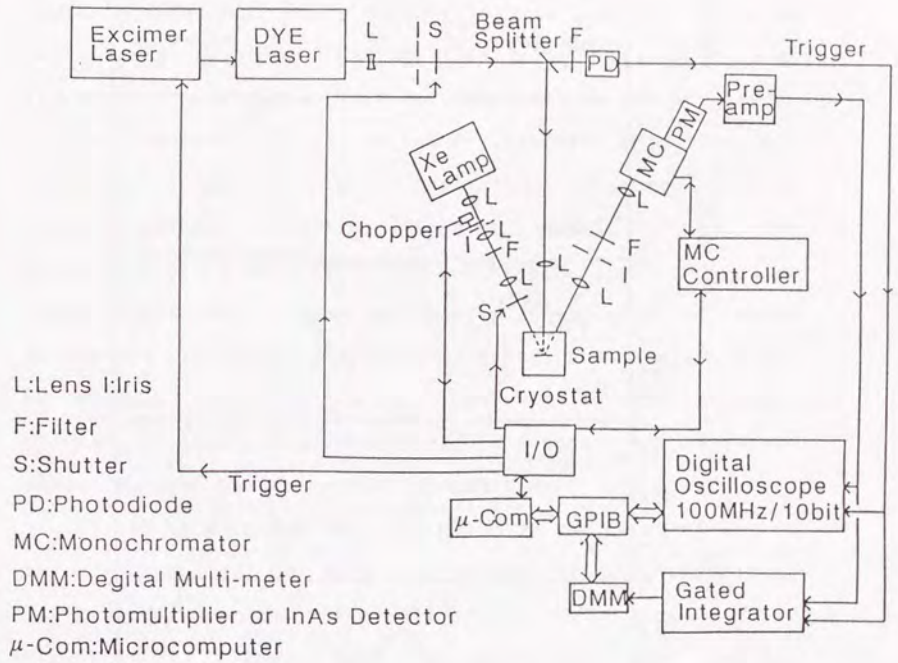

Figure II-10 : Experimental apparatus for measurement of photo-induced effects.

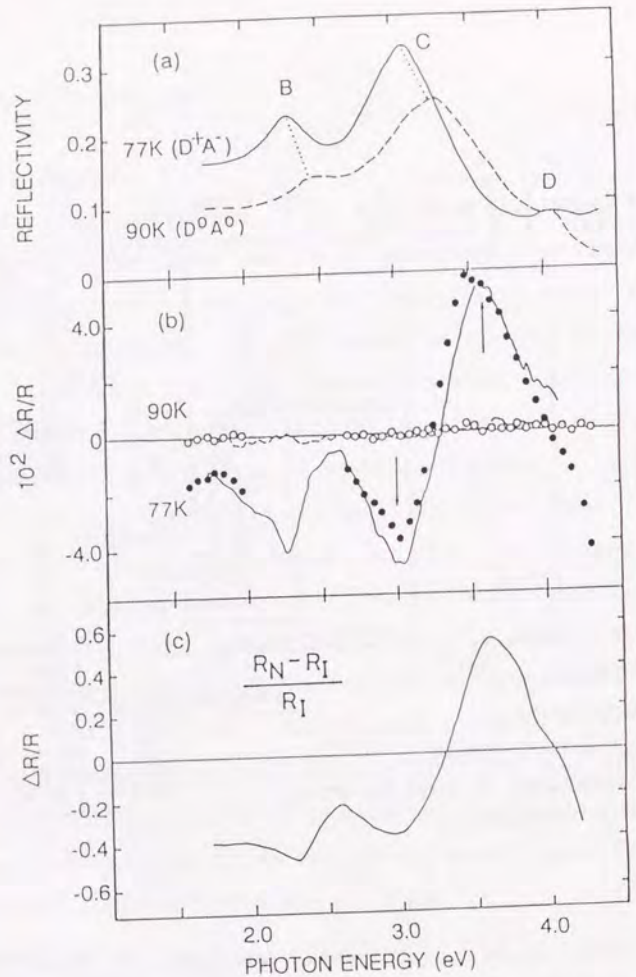

Figure II-11: Reflectance spectra (a) and corresponding photo-reflectance (PR) spectra (b) for molecular excitations (E⊥a) at 77K (I-phase) and at 90K (N-phase) in TTF-CA crystal. Ordinate scale for ΔR/R (b)is for the results for pulse-excitation shown by open (90K) and closed (77K) circles. Solid and broken lines represent the result by cw laser excitation (see text) with arbitrary ordinate scale. The spectrum (c) is the calculated differential one using the respective I-phase (R_I) and N-phase (R_N) spectra shown in (a).

spectra in the N and I phase, which were measured at 90K and 77K, respectively. PR spectra were recorded as relative difference (ΔR/R) between the spectra with and without photo-irradiation. Photo-irradiation was made at energies above the CT gap (at 2.0-2.5eV) utilizing a pulse dye laser (20ns) or a chopped light (400Hz) from a cw Ar laser. Closed and open circles in the PR spectra (Fig.II-11(b)) were the results for pulse excitation, measured with a gated-integrator (delaytime:100μs, gate-width:150μs). The both PR spectra with cw (solid and broken lines) and pulse laser light show a good agreement. In the case of pulse excitation (1.8×10^{13} photons/cm^2, 20ns), anomalously large PR signals exceeding 4% were observed in the I-phase, whereas in the N phase no detectable signal was observed under the same photo-excitation condition.

It is to be noted that the shape of the PR spectrum in the I-phase can be well reproduced by the calculated differential spectrum, {R(N)-R(I)}/R(I), which is plotted in Fig.II-11(c). Here, R(N) and R(I) are the typical reflectance spectra in the N and I phase, as shown in Fig.II-11(a). Therefore, the result indicates that the photo-excitation in the I-phase causes (semi-)macroscopic ionic-to-neutral phase conversion. In the present condition of pulse laser excitation, a fraction of the photo-converted D^0A^0-type molecular domains is estimated to amount to 11% of the sample surface at 70K. Since the attenuation depths of exciting and probing light are ca.100nm from the surface and volume of the unit cell which includes two DA pairs is equal to 812Å^3 III-1), a ratio of the number of photo-excited DA pair to the total one in the excited region is estimated to be 7×10^{-4}. Therefore, we can estimate that one absorbed

photon converts $0.11/7\times10^{-4}$ = 160 DA pairs from the quasi-ionic state to the quasi-neutral state in the surface region. It might be suspected that the observed photo-induced change would occur due to a laser-induced heating process across T_c. However, we can exclude the possibility of such a deceptive effect as discussed below.

Temperature-variation of the PR signal intensity measured at 3.0 eV (the position indicated by a downward arrow in Fig.II-11(b)) is plotted in Fig.II-12(a). The stack dimerization, which was probed by X-ray measurements[II-8] and by infrared spectra of molecular vibrations[II-3,17,18], sets in abruptly below T_c because of the spin-Peierls mechanism. At the same time, the molecular ionicity ρ jumps from ca.0.3 to ca.0.7. In accord with this NIT, PR signals are observed due to the photo-induced I-to-N conversion, but rather slowly decrease in magnitude with decrease of temperature from T_c. Even at 15K, 40% of the maximum magnitude of the PR signal was observed. If this were due to the thermal I-to-N transition via the heating above T_c(=81K) by a laser-irradiation, one would have to assume that the increase in the sample temperature were more than 70K. In that case, the similar heating would be expected in the N-phase and would cause a comparatively large PR signal above T_c even if the temperature-variation in specific heat[II-19] is taken into account. As far as a simple heating-induced NIT is assumed, it would always result in a distinct and sharp anomaly of the PR signals in a narrow temperature region around T_c. Apparently, these are not the case. The observed temperature dependence of PR signals indicates that the valence conversion over the

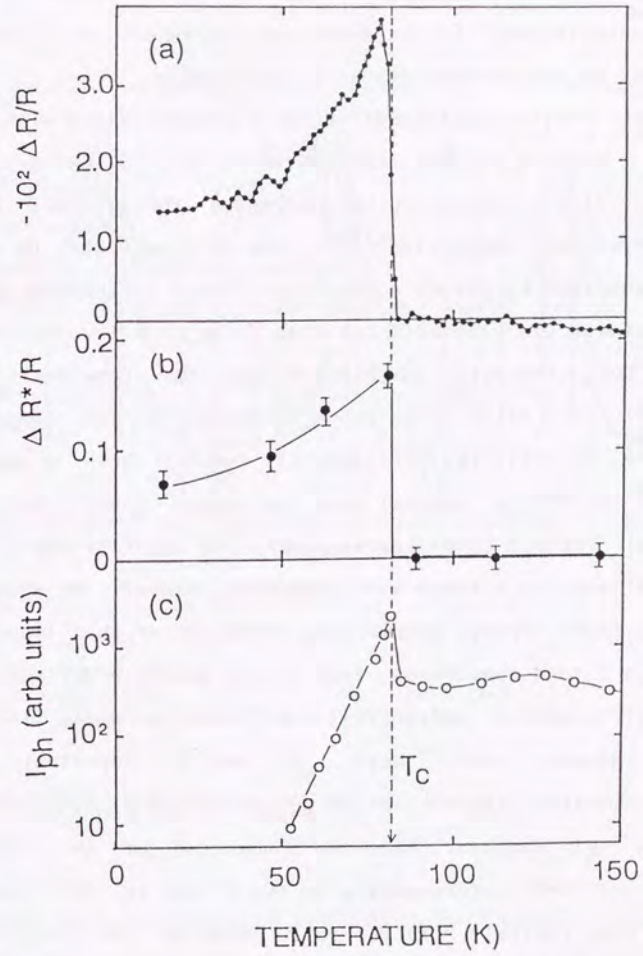

Figure II-12: Temperature dependences of the I-to-N conversion induced by photo-irradiation (a) and by impurity(QCl_3)-doping (b), and of photo-current (c). The degrees of the I-to-N changes were determined by the reflectivity changes (see text).

semi-macroscopic molecular region is evolved primarily via photo-excitations in the dimerized stacks of the I-phase, but not in the uniform stacks of the N-phase.

Such a stimulated coexistence of the N regions with the host I regions has been also observed for TTF-CA crystals doped with trichloro-p-benzoquinones (QCl_3) as site-substitutional impurities[II-20]. The QCl_3 molecule, in which one chlorine in the CA moiety (i.e. QCl_4) is hydrogenated, has a lower electron affinity than CA by ca.0.1eV and hence the QCl_3 impurity substituted for CA remains to be neutral even below T_c as shown in Fig.II-13. The important feature is that the influence of neutral QCl_3 molecules doped in TTF-CA crystal does not remain local, but the several TTF and CA molecules nearby the impurity QCl_3 are neutralized in a temperature-dependent manner. We show in Fig.II-12(b) typical temperature variation of the impurity-induced I-to-N conversion, that is the quantity defined by the differential reflectivity, $\Delta R^*/R=(R'-R)/R$, as in the photo-induced case. Here, R' and R represent the reflectivities in the the 7% QCl_3-doped (R') and undoped TTF-CA (R) samples, which were measured at the photon energy (2.5eV) corresponding to the B band in the N-phase (see Fig.II-11(a)). In the ionic phase of the QCl_3-doped crystal, the B band shows two reflectance peaks at the energy positions, 2.3 and 2.5 eV, corresponding to the I and N regions, respectively[II-20]. Therefore, the reflectivity change $\Delta R^*/R$ monitored at 2.5 eV can be a measure for the portion of the unconverted N region at temperatures below T_c. The result shows quite a parallel behavior with the photo-induced case, although the I-to-N conversion in the former case is static in nature. Such a CT instability

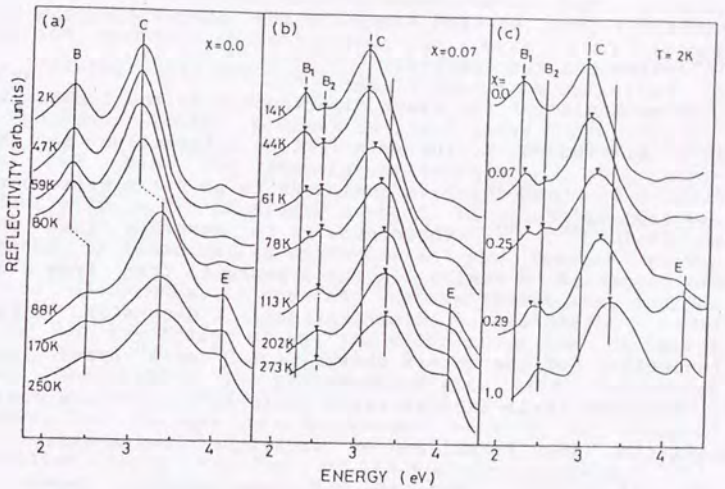

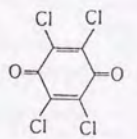

QCl_4 (CA)

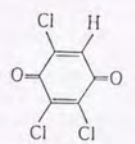

QCl_3

Figure II-13: Polarized reflection spectra of TTF-$[QCl_4]_{1-x}[QCl_3]_x$ mixed crystals for E⊥a (ref.II-20).

induced by the local impurity molecules as observed may also rationalize the present observation that a similar CT instability can be also caused by the photo-injection of $D^0(A^0)$-type charged species.

The mechanism of the stack dimerization in the I phase is likely attributed to the spin-lattice interaction in the radical D^+A^- stack which is analogous to an S=1/2 Heisenberg spin chain[II-9),14)]. Therefore, it is possible that the photo-converted N-region in the I-phase is free from the Peierls distortion (dimerization). Generally, the introduction of the excess charge (of D^0 or A^0-type) into the dimerized (Peierls-distorted) ionic (D^+A^-) lattice would result in the formation of kink-type domain-walls or solitons[II-14),21)]. Near the N-I phase boundary, however, the D^0 or A^0 type charge generates the macroscopic N-region around itself, as is evidenced by the case of A^0-type impurity doping. This is also the case for photo-generated D^0 and/or A^0 species. In such a circumstance, the concept of neutral-ionic domain-wall (NIDW), i.e. a microscopic interface separating the N-domain from the I-domain, is useful to describe the photo-electronic process. The existence of NIDW was first conjectured by Nagaosa and Takimoto[II-10)], and subsequently a number of experimental results consistent with the concept of NIDWs have been found in TTF-CA and other DA solids near the NI phase boundary[II-14,15,22 - 25)]. In this sense, the presently observed photo-induced CT instability may be interpreted in terms of the photo-doping of NIDWs. A pair of NIDW is quite analogous to the bipolaron state postulated in organic conducting polymers with two nondegenerate (stable and meta-

stable) ground states, like poly-p-phenylenes, polythiophenes, etc.[II-13)].

A part of the photo-injected NIDWs, which have escaped from the geminate recombination, can carry a fractional charge [II-10) - 12),21) - 25)] and it should be reflected in the photo-conduction process in the I-phase. In Fig.II-12(c) we plot the temperature-dependence of photo-conductivity in TTF-CA single crystal. The photo-current was measured by illuminating uniformly the gap between silver painted electrodes. A constant voltage (200V) was applied across the electrodes of ca. 1mm width along the DA stack axis. Remarkably, the photoconductivity shows anomalous increase at T_c and then decreases with a well-defined activation energy ($\simeq$ 0.09eV) at temperatures below T_c[II-24)]. The behavior cannot be explained by the laser-induced heating effect, since the dark conductivity also shows an abrupt increase by one order of magnitude on the N-to-I transition[II-14)]. It is possible that such an anomalous increase in photo-current is attributed to the photo-generation of the NIDW-type excitations originated from the photo-excited NIDWs. The activation energy of photo-current (0.09 eV) coincides with that for the dc dark conductivity, suggesting that the charge-transport phenomena both in the dark and photo-excited states are governed by the activated motion of NIDW-type excitations[II-21)].

In the I phase, most of the photo-generated neutral clusters, or equivalently pairs of NIDWs, may eventually diminish by recombination, although a part of NIDWs escape from the pair recombination and relax to the charge-carriers which contribute to the macroscopic charge transport as mentioned above. Typical results of temporal decay of

photo-generated NIDWs probed by the transient response of PR signals are shown in Fig.II-14. The PR signals were measured at photon energies of 3.0eV and 3.6 eV (indicated by arrows in Fig.II-11(a)), which monitor the photo-induced reduction of the I-region and generation of the N-domain, respectively. In accord with the expectation, the PR signals remain either negative (at 3.0 eV) or positive (at 3.6 eV), respectively, over the whole time domain. Within the time resolution (ca. 1μs) of the detection system, the magnitude of PR signals rises instantaneously after the photo-excitation, and decays rather slowly over the time region (traceably up to 10msec). Such a temporal decay can be excellently fitted by using the function, $\Delta R(t)/R = \text{Const.} \times t^{-1/2}$, over the whole time region after 20μs, as shown in Fig.II-14. An identical time-dependent behavior of PR signals is observed at other temperatures (15-70K) in the I-phase. Such a $t^{-1/2}$ behavior is known to be characteristic of the one-dimensional (1D) recombination of excited species which are randomly walking on a chain structure[II-26]. Thus, the temporal decay of PR signals reflects the 1D motion of the photo-generated NIDWs.

II-4 Conclusions

In this chapter, it was reported that a local charge-transfer (CT) excitation on the donor(D)-acceptor(A) pair leads to a semi-macroscopic valence change from the quasi-ionic to quasi-neutral state in organic molecular compound TTF-CA (see. Fig.II-15). Close correlation between photo-generated neutral-ionic domain-wall (NIDW) and photo-carrier was also confirmed. Spectroscopic studies have shown that

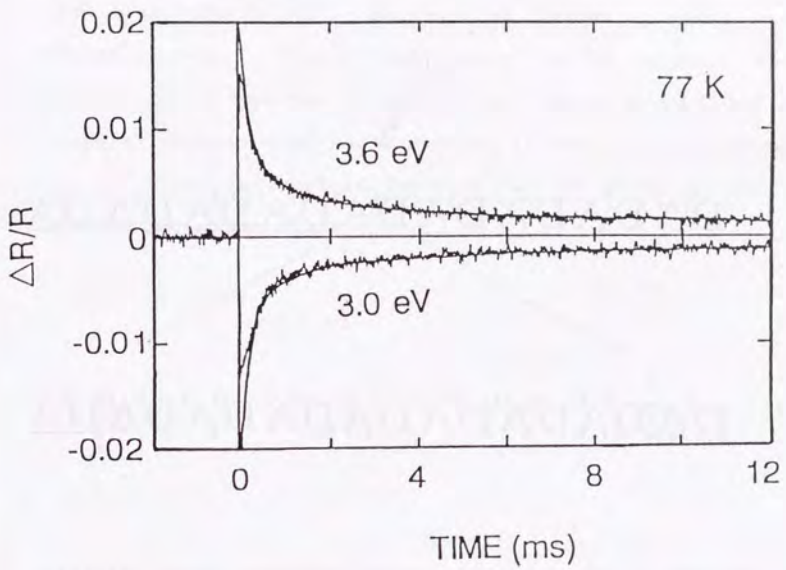

Figure II-14: Transient behavior of the photo-reflectance signals monitored at 3.0eV (for I-molecules) and 3.5eV (N-molecules) in the case of pulse laser (20ns) excitation. A smooth line represents the $t^{-1/2}$ behavior expected for the one-dimensional recombination process (see text).

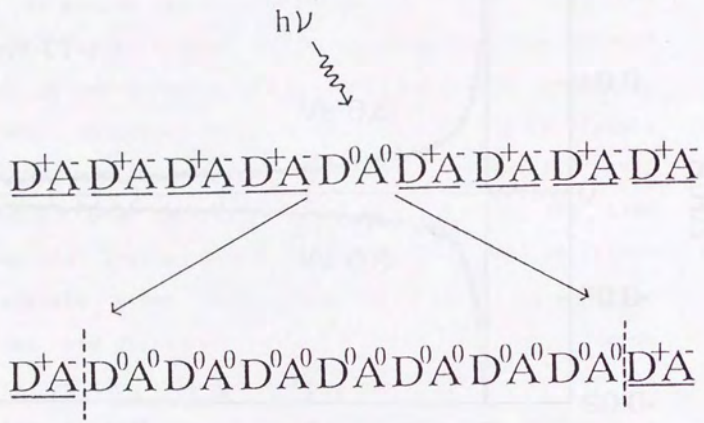

Figure II-15: Schematic for the neutral domain injection by photo-excitation observed in TTF-CA.

one absorbed photon can convert 160 DA pair from the ionic to neutral state. The temporal decay of PR signal reflects the one-dimensional motion of NIDWs toward the recombination. The initial rise of the PR signal, which could not be resolved in the present study, should reflect temporal evolution of the N-domains in the I-phase and will be of great interest in the light of the dynamics of the first-order phase transition.

REFERENCES OF CHAPTER II

II-1) J.J.Mayerle, J.B.Torrance and J.I.Crowley, Acta. Cryst. B35, 2988, (1979).

II-2) J.B.Torrance, J.E.Vazquez, J.J.Mayerle, and V.Y.Lee, Phys.Rev.Lett. 46, 253, (1981).

II-3) Y.Tokura, T.Koda, T.Mitani and G.Saito, Solid State Commun. 43, 757, (1982).

II-4) H.Okamoto, Ph. D. Thesis, The University of Tokyo, (1988).

II-5) A.Girlando, I.Zanon, R.Bozio and C.Pecile, J. Chem. Phys. 68, 22, (1978).

II-6) J.B.Torrance, A.Girlando, J.J.Mayerle, J.I.Crowley, V.Y.Lee. and P.Batail, Phys.Rev.Lett. 47, 1747, (1981).

II-7) H.M.McConnell, B.M.Hoffman and R.M.Metzger, Proc. Natl. Acad. Sci. USA, 53, 46, (1965).

II-8) Y.Kanai, M.Tani, S.Kagoshima, Y.Tokura and T.Koda, Synth. Metals, 10, 157, (1984).

II-9) J.B.Torrance, in Low Dimensional Conductors and Superconductors, NATO ASI Series B155, ed. D.Jerome and L.G.Caron, (Plenum, New York 1987).

II-10)N.Nagaosa and J.Takimoto, J. Phys. Soc. Jpn., 55, 2735, (1986).

II-11)N.Nagaosa, Ph. D. Thesis, The University of Tokyo, (1985).

II-12)Y.Tokura and N.Nagaosa, Solid State Physics, 21, 779, (1986).

II-13)For an example, Electronic Properties of Conjugated Polymers III, Springer Series in Solid-State Sciences 91, ed. H.Kuzmany, M.Mehring and S.Roth, (Springer-Verlag, Berlin 1989).

II-14)T.Mitani, G.Saito, Y.Tokura and T.Koda, Phys. Rev. Lett. 53, 842, (1984).

II-15)H.Okamoto, T.Mitani, Y.Tokura, S.Koshihara, T.Komatsu, Y.Iwasa and T.Koda, Phys. Rev. B in press.

II-16)Y.Iwasa, T.Koda, S.Koshihara, Y.Tokura, N.Iwasawa and G.Saito, Phys. Rev. B 39, 10441, (1989).

II-17)A.Girlando, C.Pecile, A.Brillante and K.Syassen, Solid State Commun. 57, 891, (1986).

II-18)A.Girlando, F.Marzola and C.Pecile, J. Chem. Phys. 79, 1075, (1983).

II-19)C.Ayache and J.B.Torrance, Solid State Commun. 47, 789, (1983).

II-20)Y.Tokura, T.Koda, G.Saito and T.Mitani, J. Phys. Soc. Jpn. 53, 4445, (1984).

II-21)Y.Tokura, S.Koshihara, Y.Iwasa, H.Okamoto, T.Komatsu, T.Koda, N.Iwasawa and G.Saito, Phys.Rev.Lett. 63, 2405, (1989).

II-22)Y.Tokura, H.Okamoto, T.Koda, T.Mitani and G.Saito, Physica 143B, 527, (1986).

II-23)T.Mitani, Y.Kaneko, S.Tanuma, Y.Tokura, T.Koda and G.Saito, Phys.Rev.B, 35, 427, (1987).

II-24)T.Mitani, Y.Tokura, Y.Kaneko, K.Takaoka, T.Koda and G.Saito, Synth. Metals,19, 515, (1987).

II-25)Y.Tokura, H.Okamoto, T.Koda, T.Mitani and G.Saito, Phys. Rev. B, 38, 2215, (1988).

II-26)C.V.Shank, R.Yen, R.L.Fork, J.Orenstein and G.L.Baker, Phys. Rev. Lett. 49, 1660, (1982).

CHAPTER III

Inverse Peierls Transition Induced by Photo-excitation in potassium-tetracyanoquinodimethane (K-TCNQ)

III-1 INTRODUCTION

In this chapter, we deal with a simple radical salt, alkali-metal(potassium)-tetracyanoquinodimethane (TCNQ) (hereafter abbreviated as K-TCNQ). K-TCNQ is composed of quasi-one-dimensional columns (along the a-axis) of TCNQ molecules as shown in Fig.III-1)[III-1,2]. The charge transfer between TCNQ and K is complete ($K^{+\rho}$ $TCNQ^{-\rho}$: ρ=1). The transferred electrons are strongly localized due to larger value of the on-site electron-electron Coulomb repulsion energy (U≃1.4 eV) than that of the transfer (t≃0.2 eV)[III-3]. Crystals of K-TCNQ undergoes the first order phase transition accompanying the change in magnetic susceptibility [III-4] (see Fig.III-2) and the stack-dimerization or Peierls-distortion [III-1,2,5] (see Fig.III-3 and 4) at T_c=395K like the other crystals of alkali-TCNQ family. In low temperature phase, the intra-dimer distance is ca. 5% shorter than the inter-molecular spacing of homogeneous stack (in the high temperature phase)[III-1]. The dimerization of molecular sites alternately modulates the electron transfer energy (t) and hence causes a sort of bond-ordered-wave (BOW) similar to the conjugated polymer polyacetylene [III-6]. When U>>t, the regular $TCNQ^-$ stacks can be considered to be s=1/2 Heisenberg chain with anti-ferromagnetic exchange interaction J ($\simeq 4t^2/U$) as shown in Fig.III-5. In this sense, the observed phase transition is analogous to the spin-Peierls transition [III-7 - 9] although the energy scale

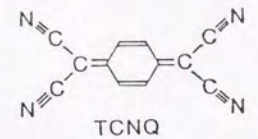

TCNQ

Lattice Constants

at 298K	at 413K
a=7.0835Å	a=3.587Å
b=17.773Å	b=12.676Å
c=17.859Å	c=12.614Å
β=94.95deg	β=96.44deg
Z=8	Z=2

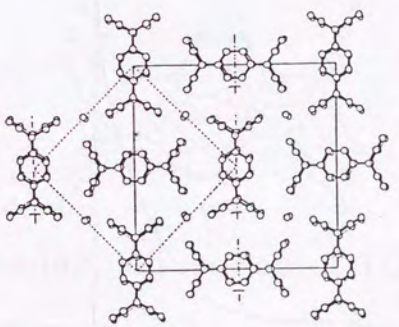

Projection along the a axis onto (100) plane

Figure III-1 : Structure and lattice parameters of K-TCNQ in high and low temperature phases. Solid, and broken lines indicate the unit cells in low, and high temperature phases, respectively (ref.III-1 and 2).

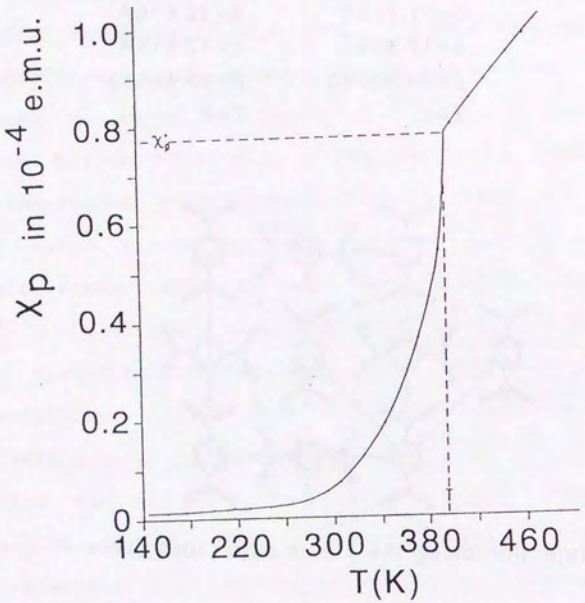

Figure III-2 : Temperature dependence of the molar paramagnetic susceptibility χ_p of K-TCNQ (ref.III-4).

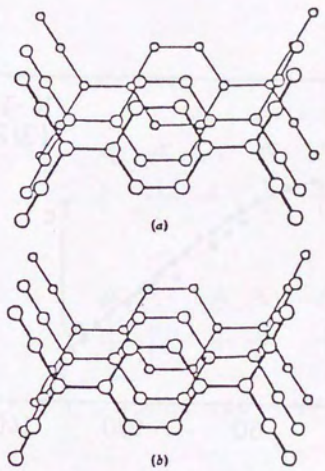

Overlapping modes of $TCNQ^-$ units

(a) Low-temperature phase

(b) High-temperature phase

Figure III-3 : Overlapping modes of $TCNQ^-$ units in low (a) and high (b) temperature phases (ref.III-1).

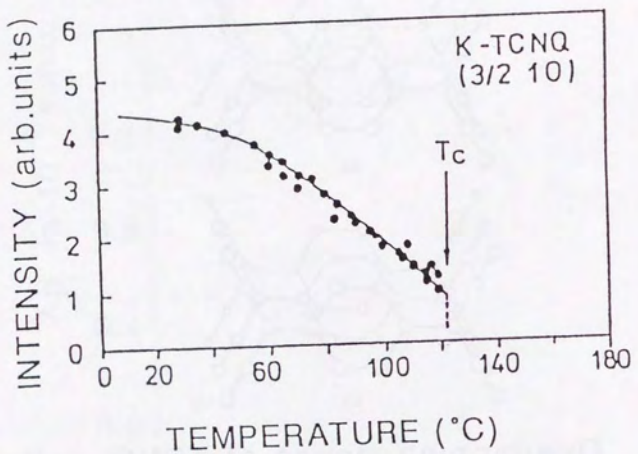

Figure III-4 : Temperature dependence of the intensity of the superlattice reflection in K-TCNQ (ref.III-5).

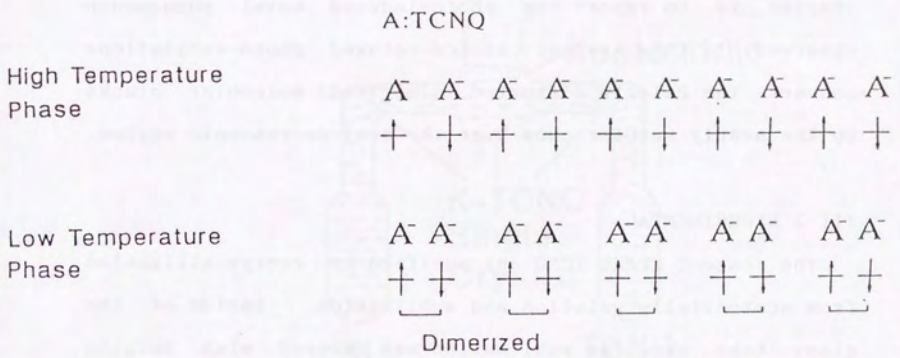

Figure III-5 : Schematic for electronic structure of K-TCNQ crystal in the high and low temperature phases.

of J is considerably large (≃0.1 eV) in K-TCNQ as compared with the case of prototypical spin-Peierls systems[III-2].

Considering these features, alkali-TCNQ crystals are appropriate materials to investigate the behavior of photo-injected carriers in the half-filled Hubbard system with strong electron-lattice interaction. The purpose of this chapter is to report the photo-induced novel phenomenon observed in this system: Lattice-relaxed photo-excitations convert the Peierls distorted (dimerized) molecular stacks to the nearly regular ones over the semi-macroscopic region.

III-2 EXPERIMENTAL

The reagent grade TCNQ was purified by recrystallization from acetonitrile solution and sublimation. Inside of the glass tube used for sublimation was covered with tefulon seat to prohibit reaction between TCNQ molecules and metalic ions in the glass. Single crystals of K-TCNQ were grown by the conventional liquid-phase reaction of the constituent cation (K^+) and $TCNQ^-$ radical anion through diffusion in the acetonitrile solution at ca. 290 K (see Fig.III-6). As the starting materials, reagent grade powders of KI were used. After the reaction which took about 20 days, needlelike single crystals, of which typical size was about 10x1x1 mm^3, were obtained [III-10].

Photo-induced reflectance (PR) spectra of single crystals in visible and near IR regions as well as their time-dependences have been measured by the conventional pump-probe system using excimer pumped pulsed dye laser which is shown in Fig.II-10. The PR spectra were recorded by a box-car integrator with the delay-time of 3μs and the gate-width

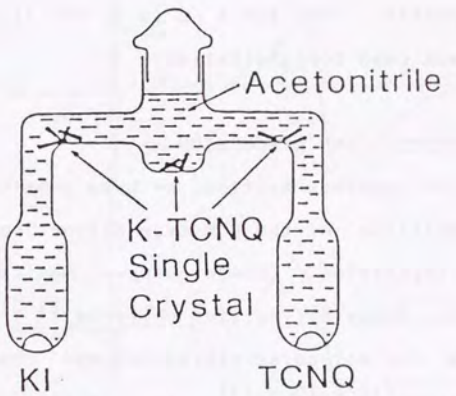

Figure III-6 : Synthesis of K-TCNQ single crystals by liquid-phase reaction using U-tube.

of 5μs. The photon energy, and pulse width of dye laser was 2.1 eV, and 20 ns, respectively. Typical resolution time of this system was 500 ns. The differential spectra with and without laser irradiation in molecular vibrational region has been observed for the polycrystalline samples dispersed in KBr pellets using a Fourier-transform-type spectrometer. The 514.5 nm (2.41 eV) light from cw Ar ion laser was used for excitation.

III-3 RESULTS AND DISCUSSION

In the previous section, we have mentioned that change in the amplitude of the BOW-type distortion occurs upon the phase transition. These changes manifest themselves not only in X-ray diffraction patterns[III-5], but in optical spectra for molecular vibrations and charge-transfer (CT) excitations[III-3,10 - 14]. In Fig.III-7(a), we show the optical absorption spectra for the low-temperature phase (measured at 293K) and for the high-temperature phase (at 409K). The vibrational spectra were measured on the polycrystalline samples dispersed in KBr pellets, while the absorption spectra for the CT excitation ($TCNQ^{-1}$ + $TCNQ^{-1}$ -> $TCNQ^{0}$ + $TCNQ^{-2}$) were obtained by Kramers-Kronig analysis of the polarized (E//a) reflectance spectra of single crystal. The CT band in the low-temperature phase shows the maxima (A) around 1.0 eV and the side-band (B) around 1.4eV as shown in the right part of Fig.III-7(a). Most simply, the splitting of the band can be ascribed to coexistence of intra- and inter-dimer CT excitations in the low-temperature BOW phase[III-14], although other possible origins of this doublet structures were proposed in literatures[III-3,13,15] Upon the phase transition the magnitude of the CT gap

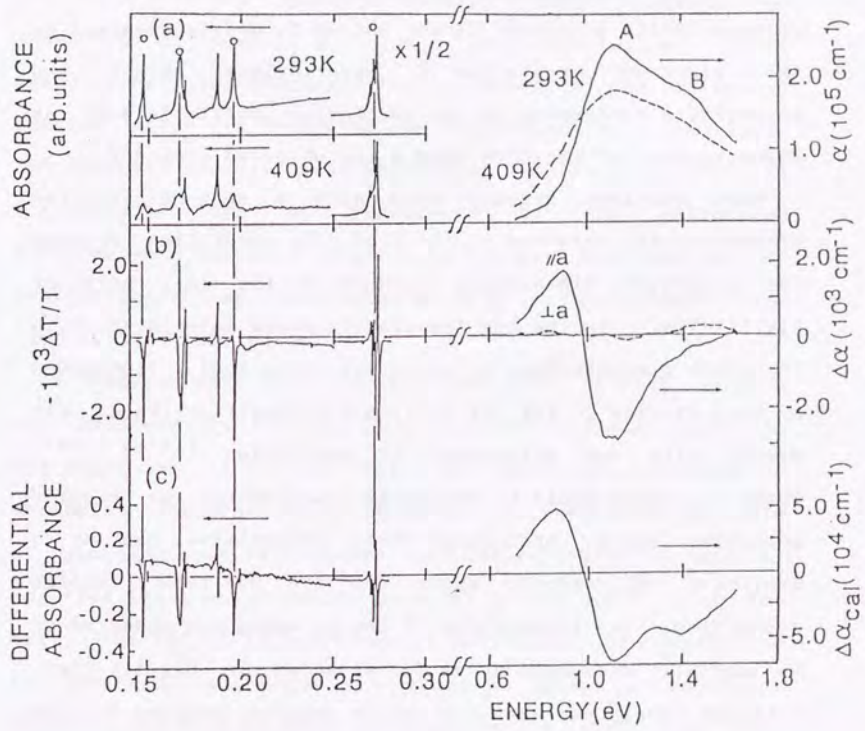

Figure III-7 : Spectra of (a) absorption, (b) photo-induced absorption, and (c) simulated differential absorption for molecular vibrations (left) and charge-transfer excitations (right) of K-TCNQ. The absorption and photo-absorption bands of a_g vibrations are indicated by open circles. Solid and broken lines in the right part of (b) represent the polarized photo-absorption spectra for E//a (stack-axis) and for E a, respectively.

changes little since the CT gap energy is mostly governed by the electron correlation U, nevertheless abrupt and appreciable broadening of the absorption profile as well as disappearance of the side-band B are observed around T_c.

More distinct changes upon such a spin-Peierls-like transition are observed in infrared (IR) absorption spectra for molecular vibrations, as shown in the left part of Fig.III-7(a). In the low-temperature phase associated with the stack dimerization, a_g molecular vibrations (indicated by open circles in Fig.III-7(a)) are strongly activated via mixing with the electronic CT excitation [III-15 - 20]. These a_g modes would be optically inactive for the regular molecular stack, and hence their intensities can be a sensitive microscopic probe for the BOW-type lattice distortion. The intensities of the a_g modes are observed to be abruptly decreased above Tc, as shown in Fig.III-7(a), although their residues are barely observed perhaps due to the 1D fluctuation effect[III-14].

Keeping the above in mind, let us proceed to experimental results of photo-induced changes of vibrational and CT excitation spectra shown in Fig.III-7(b). What we have observed here is that a pulse or cw laser irradiation on K-TCNQ crystal with the dimerized stacks (BOW) produces a mesoscopic size of molecular domains with nearly regular (non-BOW) stacks.

In the left of Fig.III-7(b) is shown the differential spectrum between with and without laser irradiation at 293K ($<T_c$) in molecular vibrational region. Typical laser intensity was 300mW/cm^2 on the sample surface of KBr pellets and the absorbed light power was estimated to be ca.

100 W/cm^3. The spectrum clearly shows decrease in intensity of each a_g band upon photo-excitation. This means that the photo-excitation produces the molecular domains which are free from the BOW distortion. In fact, the observed photo-induced absorption (PA) spectrum shown in Fig.III-7(b) can be reproduced by the calculated differential spectrum (Fig.III-7(c)) which are obtained by subtracting the spectrum taken at 409K (non-BOW phase) from that at 293K (BOW phase).

A considerable photo-induced change of optical spectra was observed also for the CT excitation region as shown in the right part of Fig.III-7(b). The photo-induced change of absorption spectra were obtained by Kramers-Kronig analysis of photo-induced reflectance (PR) change ($\Delta R/R$) in sample. For the light polarization parallel to the stack axis (a-axis) the fairly large change of reflectance or absorbance is observed, while the E$\perp$a spectrum shows no prominent signal. The E//a PA spectrum shown in Fig.III-7(b) is well reproduced by the calculated differential absorbance spectra shown in Fig.III-7(c). The behavior is consistent with the above-mentioned observation about the photo-induced change of IR vibrational spectra : The both results indicate that the photo-excitation in the BOW phase of K-TCNQ generates the molecular states analogous to the high temperature phase. These photo-induced changes are not due to the simple irradiation-induced heating, which is evidenced by their temperature-dependent behaviors as described later.

As an advantage of the pulse excitation experiment, we can estimate size of photo-converted molecular domain and observed its temporal change. In Fig.III-8 are plotted the photo-induced reflectivity change ($\Delta R/R$) detected at 1.1eV

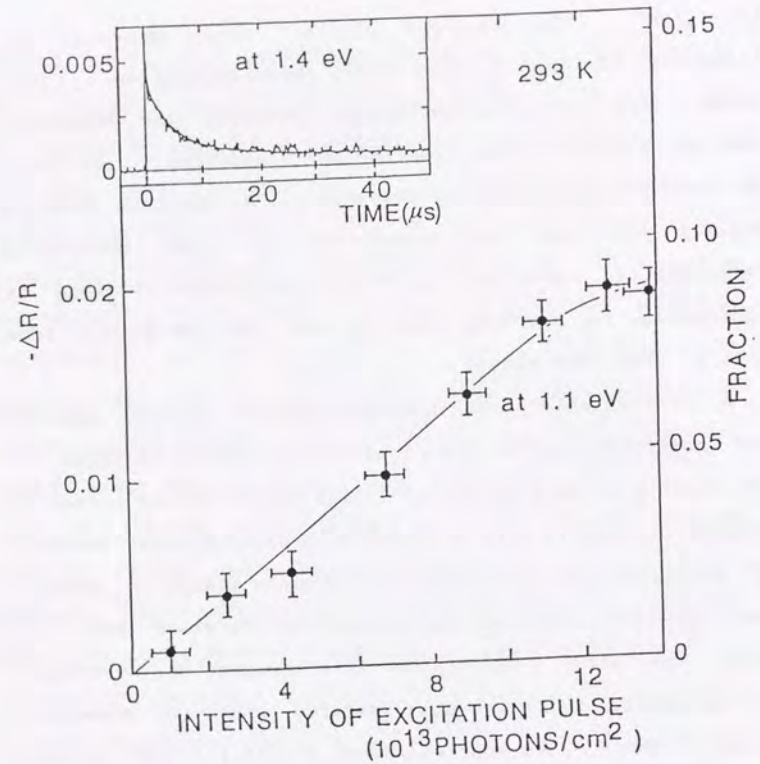

Figure III-8 : Dependence of photo-reflectance (PR) signals (monitored at 1.1eV) on the intensity of exciting light (E//a, 2.1eV, and 20ns duration) at 290K. Scale of the right ordinate indicates the fraction of photo-converted molecular region (see text). In the inset is shown the time-dependence of PR signal at 1.4eV. A smooth thin line in the inset represents the $t^{-0.5}$ behavior expected for the one-dimensional recombination process.

against the photon density at the crystal surface. The right ordinate indicates the fraction of the photo-converted non-BOW molecular domains to the background BOW lattice. The converted fraction could be estimated by assuming that the exciting and probing light penetrate the same depth (d_{skin}) of ca.140nm from the surface and that the observed spectrum is well approximated by the differential spectrum between the high-temperature non-BOW phase and the low-temperature BOW phase. (See Fig.III-7(b) and (c).) The magnitude of $\Delta R/R$ or equivalently the converted fraction (F) of the non-BOW region is approximately proportional with the exciting light intensity I_e, as far as I_e does not exceed $1x10^{14}$ photons/cm^2. Using the density (n_{TCNQ}) of $TCNQ^-$ molecules ($3.6x10^{21}$/cm^3) in K-TCNQ crystal[III-1], we can estimate the size of the non-BOW molecular domain, which is generated by one absorbed photon, as follows;

$$\frac{n_{TCNQ} \times F \times d_{skin}}{I_e}$$

The domain size was estimated to be over ca.40 $TCNQ^-$ molecules under the present condition. This estimation was the most modest, since we have assumed that <u>all</u> the photo-excited species can take part in causing the inverse-Peierls-like transition with <u>100%</u> efficiency.

In the inset of Fig.III-8, we show a typical trace of temporal decay of photo-induced signal, which should represent the temporal disappearance of photo-converted non-BOW domains. The time-dependence of the signal is excellently fitted by the $t^{-1/2}$-curve as shown by a smooth thin line in the figure. This indicates that the photo-converted molecular domains extinguish by recombination of a

pair of domain-walls (DWs) which are randomly walking on the 1D stack[III-21].

It might be suspected that the observed semi-macroscopic change of the lattice structure induced by photo-excitation were simply due to the temperature increase of the sample surface region across T_c. However, we can exclude the possibility of such an artifact by following experimental observations. In Fig.III-9(a) is plotted the temperature-variation of the photo-induced signal ($\Delta R/R$) by a solid line. Closed squares represent the result for the bleaching degree of the 1570cm^{-1} a_g molecular vibration by a cw laser excitation (see the left part of Fig.III-7(b)). In spite of a large difference in absorbed light power per unit volume between the two cases (100W/cm^3 for cw excitation and 5W/cm^3 for pulse excitation operated at 5Hz), the both results show an essentially identical temperature-dependence: The photo-conversion efficiency increases with temperature up to 330K, but then begins to decrease as temperature goes towards T_c. Around T_c the photo-induced signals are observed to disappear. Such a temperature-dependence cannot be explained by the laser-induced heating of the sample surface. If it were the case, the photo-induced change would be strongly enhanced around T_c due to the first order character of the phase transition. To demonstrate this, the temperature dependence of the PR signal was simulated assuming the laser-induced heating with temperature increase of 10K. (For this calculation, the observed temperature dependence of reflectivity at 1.2 eV was used.) The result, which is shown by a broken line in Fig.III-9(a), is entirely different from the observed temperature-variation of PR.

In Fig.III-9(c), we reproduce, for comparison, the

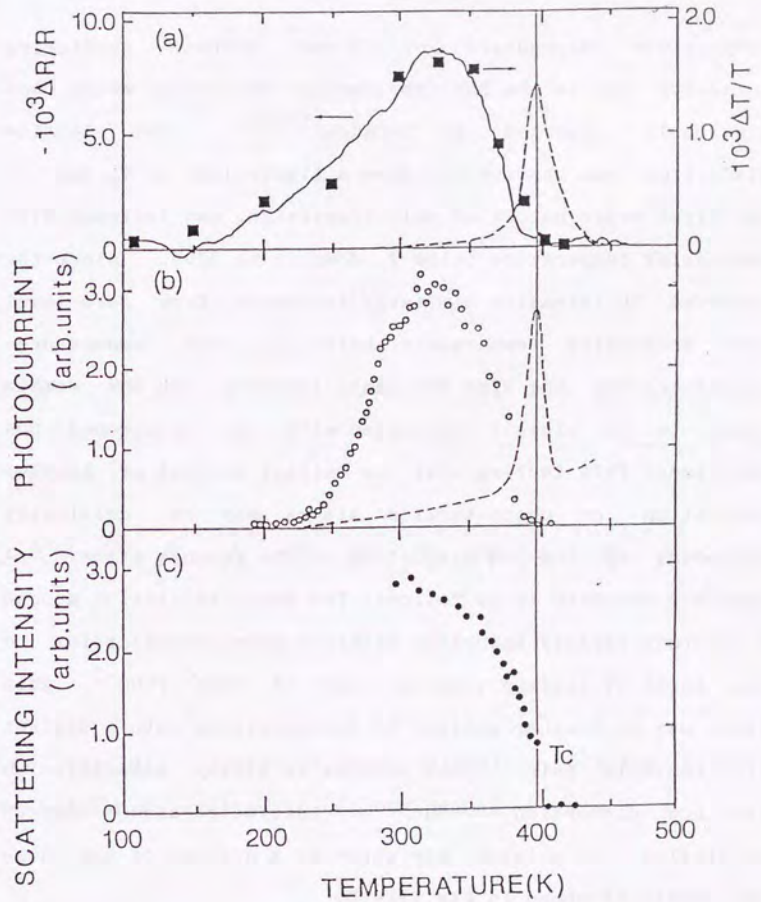

Figure III-9 : Temperature-dependences of (a) photo-reflectance signal at 1.2eV (a solid line) and absorbance change of the 0.195eV (1570cm^{-1}) a_g mode (closed squares), (b) photo-current (open circles), and (c) X-ray diffuse diffraction intensity due to the dimeric lattice distortion reported by Terauchi[III-5]. Broken lines in (a) and (b) represent the simulated result assuming the irradiation-induced heating of the sample (see text).

temperature dependence of X-ray diffuse scattering intensity due to the BOW-type lattice distortion which was previously reported by Terauchi[III-5]. The lattice distortion was observed to show a finite jump at T_c due to the first order nature of this transition, and increase with decreasing temperature below T_c down to ca.300K. Since the observed PR intensity similarly increases from zero-level with decreasing temperature below T_c, the temperature-dependence of the size of photo-injected non-BOW domain seems to be closely correlated with the background BOW amplitude. This implies that the initial process of lattice relaxation of photo-excited states may be critically dependent on the BOW distortion of the ground state. A possible scenario is as follows: The photo-excitation around 2.1eV may rapidly (probably within a pico second) relax to the local CT exciton such as a pair of $TCNQ^0$-$TCNQ^{-2}$. This state may be further subject to decomposition into a distant electron-hole pair. This process is likely sensitive to the BOW distortion. Such a lattice-relaxed charged excitation, or polaron, may serve as a nucleus of the non-BOW domain as shown in Fig.III-10.

In this context, it is worth noting that the temperature-dependence of photo-current (Fig.III-9(b)) exhibits quite a parallel behavior with that of the PR signal except for the low-temperature region below 250K. The photo-current was measured for the 2.1eV pulse laser excitation (as in the PR measurement) with application of dc electric field (200 V/cm) along the a-axis (stack-axis). The signal is not due to the simple heating effect, such as photo-voltaic effect. Also in this case, the simulated curve (a broken line in

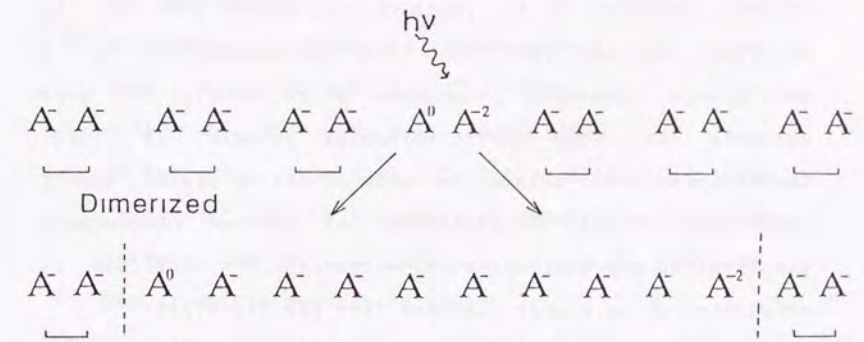

Figure III-10: Picture of model relaxation process from photo-induced CT exciton to non-BOW domain.

Fig.III-9(b)), which was calculated with dc conductivity data assuming the irradiation-induced temperature increase of 10 K, is entirely different from the observed one. Nearly identical thermal variation of the PR and photo-conduction data suggests that the photo-converted non-BOW domains or their domain-walls can carry electric charge. A steeper decrease of the photo-current below 300K may be ascribed to the fact that the photoconduction is a macroscopic transport phenomenon which should be more amenable to some carrier-trapping process at lower temperatures. The gradual decrease of the PR signal itself below 300K should be explained by another microscopic deactivation process, since below 300K the BOW-amplitude is considered to be nearly constant (see Fig.III-9(c)).

III-4 Conclusion

In this chapter, we have investigated the photo-induced inverse-Peierls like transition in K-TCNQ crystal over a mesoscopic size of molecular domain (at least 40 molecules per one absorbed photon). Of course, the photo-injected domain is not stable in this case and the observed photo-induced effect in K-TCNQ is not literally 'photo-induced phase transition'. The photo-converted domains or their domain-walls between the BOW and non-BOW regions can likely carry electric charge which is observed as a photo-current. The precursory excitation for such a phase conversion is not clear at present, but is presumably the lattice relaxed CT excitons or dissociated polarons which can switch off the collective channel of electron(spin)-lattice interaction characteristic of this 1D system.

REFERENCES OF CHAPTER III

III-1) M.Konno, T.Ishii and Y.Saito, Acta Cryst. Sec.B 33, 763, (1977).

III-2) "Extended Linear Chain Compounds" vol III ed. by J.S.Miller (Plenum New York 1983).

III-3) K.Yakushi, T.Kusaka and H.Kuroda, Chem. Phys. Lett. 68, 139, (1979).

III-4) J.G.Vegter, T.Hibma and J.Kommandeur, Chem. Phys. Letters, 3, 427, (1969).

III-5) H.Terauchi, Phys. Rev.B 17, 2446, (1978)

III-6) "Electronic Properties of Polymers and Related Compounds" Ed. by H.Kuzmany, M.Mehring and S.Roth, Springer Series in Solid-State Science 63 (Springer-Verlag Berlin Heiderberg 1985).

III-7) Y.Lepine, A.Caille and V.Larochelle, Phys. Rev.B 18, 3585, (1978).

III-8) Y.Takaoka and K.Motizuki, J. Phys. Soc. Jpn. 47, 1752, (1979).

III-9) Y.Lepine, Phys. Rev.B 28, 2659, (1983).

III-10) H.Okamoto, Ph. D. Thesis, The University of Tokyo (1988).

III-11) Z.Iqbal, C.W.Christoe and D.K.Dawson, J. Chem. Phys. 63, 4485, (1975).

III-12) R.Bozio and C.Pecile, J. Chem. Phys. 67, 3864, (1977).

III-13) K.Yakusi, S.Miyajima, T.Kusaka and H.Kuroda, Chem. Phys. Lett. 114, 168, (1985).

III-14) H.Okamoto, Y.Tokura and T.Koda, Phys. Rev.B 36, 3858, (1987).

III-15) D.B.Tanner, C.S.Jacobsen, A.A.Bright and A.J.Heeger, Phys. Rev.B 16, 3283, (1977).

III-16) M.J.Rice, Phys. Rev. Lett. 37, 36, (1976).

III-17)M.J.Rice, N.O.Lipari and S.Strassler, Phys. Rev. Lett. 39, 1359, (1977).

III-18)M.J.Rice, Solid State Commun. 31, 93, (1979).

III-19)S.Etemad, Phys. Rev.B 24, 4959, (1981).

III-20)A.Painelli and A.Girlando, J. Chem. Phys. 84, 5655, (1986)

III-21)C.V.Shank, R.Yen, R.L.Fork, J.Orenstein and G.L.Baker, Phys. Rev. Lett. 49, 1660, (1982).

CHAPTER IV

Reversible and Irreversible Thermochromic Phase Transitions in Single Crystals of Polydiacetylenes Substituted with Alkyl-urethanes

IV-1 INTRODUCTION

Polydiacetylenes (PDAs) ($\{CR-C\equiv C-R'C\}_x$) have been extensively studied for their unique π-electronic properties, such as a drastic color change by various stimulations[IV-1 - 7] and large nonlinear optical susceptibilities[IV-1,8 - 10] with an ultrafast response time[IV-9]. The one-dimensional conjugated backbone structures coupled with side groups (R and R') are responsible for these unique characters. By suitable selections of side groups, PDAs can be obtained in various forms including high quality single crystals, Langmuir-Blodgett films, vaccum-deposited films, and solutions or gels. Systematic modifications in side groups also enable us to enhance those noble properties and to develop new ones with useful functionalities.

The PDAs investigated here have alkyl-urethane side-groups ($R=R'=(CH_2)_4OCONH(CH_2)_{n-1}CH_3$) with various lengths of alkyl chain (n=1-10) as shown in Fig.IV-1. Hereafter, this new family of PDAs and corresponding monomers are abbreviated as poly-4Un and mono-4Un, respectively. Two kinds of alkyl chains in the side-group are denoted as inner and outer alkyl chains according to distance from the polymer backbone (see Fig.IV-1). Among the poly-4Un series, poly-4U2 (ETCD) has been well known for its reversible thermochromic change between the two spectroscopically

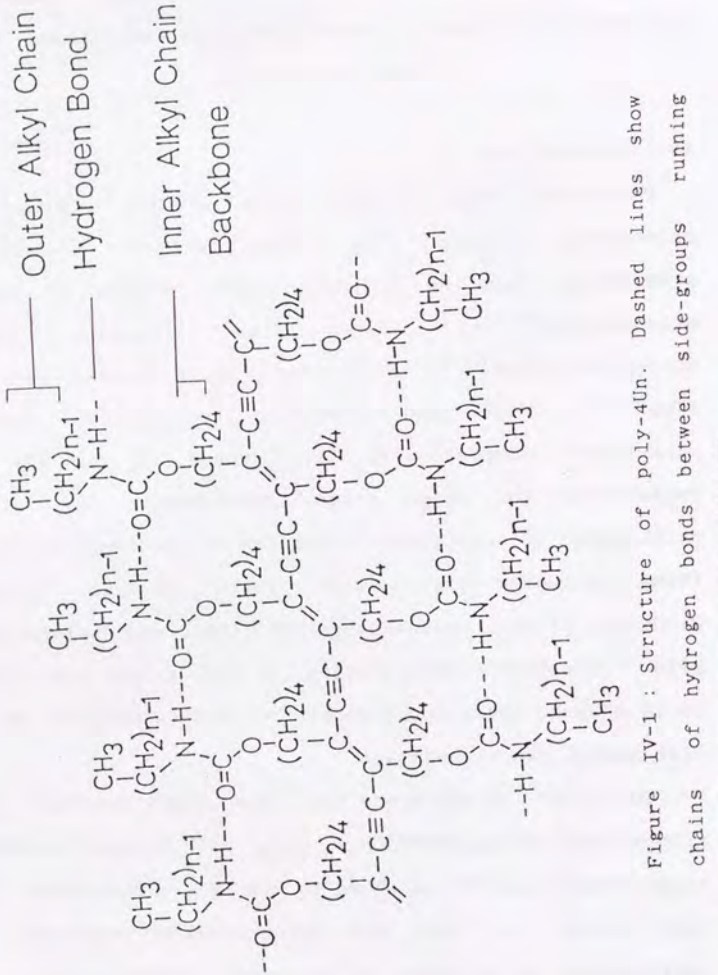

Figure IV-1 : Structure of poly-4Un. Dashed lines show chains of hydrogen bonds between side-groups running parallel to the polymer backbones.

distinct forms [IV-2], A(blue)- and B(red)-forms (see Fig.IV-2), and extensive studies have been made on the correlation between conjugated backbone structures and conformations of side-groups [IV-11 - 14]. At the early stage of the study, it was postulated that the hydrogen bonds might play a crucial role in triggering the thermochromic phase transition, but Rubner et al.[IV-12] have recently shown that the interruption of the hydrogen bond chains in the side-groups does <u>not</u> occur in poly-4U2 (ETCD) during the reversible thermochromic A-B transition. More lately, Tanaka et al.[IV-13] have found from results of ^{13}C NMR measurements that a 'trans-gauche'-like conformational change in the inner alkyl chain occurs during the reversible thermochromic change in poly-4U2 (ETCD). On the other hand, it was reported that the B-phase is stabilized even at room temperature when disorder in hydrogen bond is caused by gentle thermal treatment in thin films of ETCD [IV-6]. In this context, the present study on the poly-4Un series is a natural extension of the previous studies on poly-4U2 (ETCD) and may provide a broader perspective on the notable feature of reversible and irreversible chromatic phase transitions in PDAs. In addition, a family of poly-4Un are also of current interest, because the n=3-5 materials are quite suitable for a fabrication of highly oriented thin films which can show a large nonlinear optical susceptibility [IV-10].

In the next chapter (V), we will show that the reversibly photo-induced phase transition is observed for the first time on one of the poly-4Un crystals (n=3). This chapter is devoted, as a preceding investigation, to characterization of this new family of PDAs and their

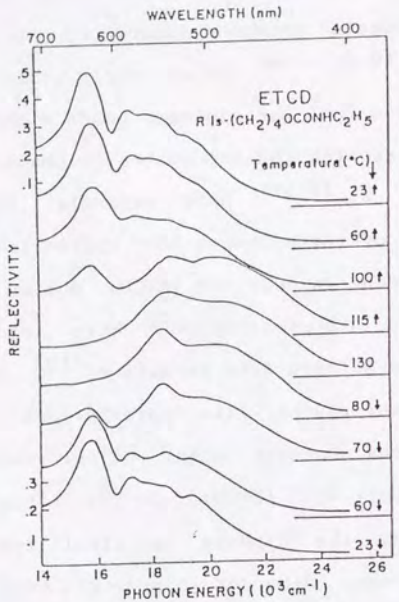

Figure IV-2 : Reflectance spectra of ETCD (poly-4U2) as a function of temperature (ref. IV-2).

thermally-induced phase transition.

In the following, we will show that both reversible and irreversible thermochromic transitions are observed for all poly-4Un's (n=1-10). We have investigated changes in the electronic and lattice structures upon the phase transitions by means of measurements of IR-visible absorption, reflectance, Raman and fluorescence spectra as well as of X-ray diffraction and calorimetric thermograms.

IV-2 EXPERIMENTAL

Alkyl-urethane di-substituted diacetylene monomers (mono-4Un) with n=1-10 were prepared by the following method: 1 ml di-n-butyltin dilaurate were added to 50 ml of ethereal solution of 5,7-dodecadiyne-1,12-diol(1.0×10^{-2} mol) and of corresponding n-alkylisocyanate (2.2×10^{-2} mol), and the mixture was kept stirring overnight at room temperature. After removing ether, the residue (mono-4Un) was washed with n-hexane and purified by the recrystallization from ethylacetate. Monomer single crystals for n=2 to 5 have been obtained by slow evaporation of ethyl acetate solution with sizes of 1x3x0.1 mm, 3x10x1 mm, 0.8x0.8x0.1 mm, and 0.5x0.5x0.1 mm for n=2, 3, 4, and 5, respectively. For other n's (n=1,6-10), only microcrystalline powders were obtained. Monomer crystals were polymerized by gamma-ray irradiation with dose of 60 Mrad. To estimate the degree of polymerization, we tried to extract the unreacted monomers using acetone from the finely ground samples. The measurements for weight-loss of the residue as well as for the UV spectrum of extraction solvent indicated that the quantity of the unreacted monomers was less than the

detection limit (ca. 2%) for the n=3, 4 and 5 polymers. For the other samples with n=1, 2, 6-10, the sample quantity was not sufficient to do the extraction studies, but their DSC thermograms indicated that there is at least no bulk quantity of unreacted monomers.

To observe the chromatic change, reflectance spectra were measured on (100) surface of single crystal in the condition of nearly normal incidence. Data of fluorescence and Raman spectra were taken by use of the conventional photon-counting system coupled with a double monochromator and cw Ar-ion laser in the back scattering configuration. The spectral response of the detection equipment was corrected. Measurements of infrared vibrational modes were made on polycrystalline powder dispersed in KBr pellets. During the optical measurements, temperatures of samples were kept nearly constant within $\pm$0.5 K.

Temperature-dependence of lattice constants of crystal was measured by an X-ray diffractometer equipped with a temperature-controlled sample holder. At room temperature, Weissenberg photographs were also taken on single crystals to check the consistency of the lattice parameters with those determined by the powder diffraction method.

IV-3 RESULTS AND DISCUSSION

IV-3-1 Overview of thermochromic changes in poly-4Un family

Before going to detailed discussion on the experimental results and on the mechanism of phase transitions, we present overall features of the thermochromism and relevant phase-diagram in the poly-4Un series. First, we show in Fig.IV-3 some examples of the dichroism observed by

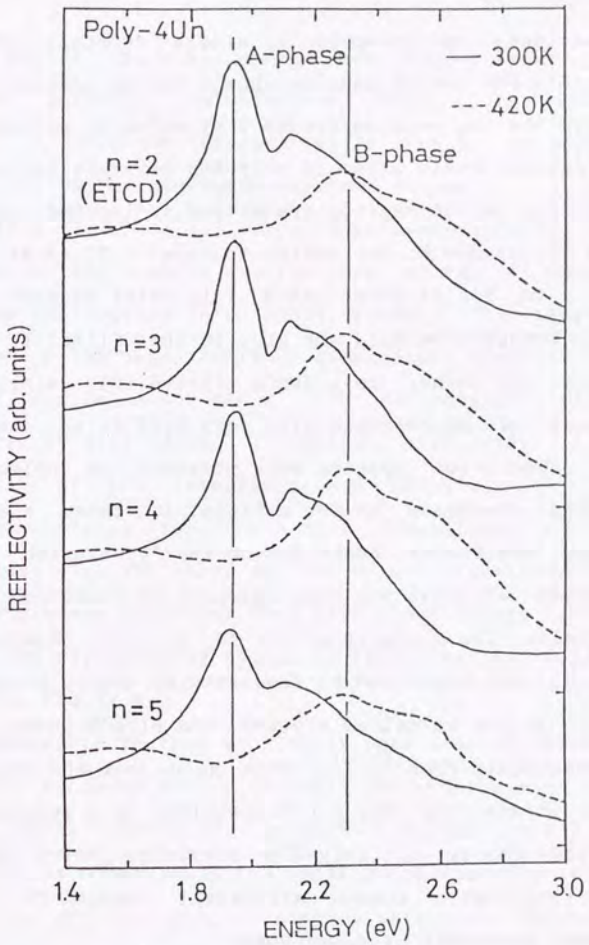

Figure IV-3 : Reflectance spectra of poly-4Un single crystals with n=2, 3, 4 and 5 in the A- (solid line) and B- (dashed line) phases. The spectra in the A- and B-phases were measured at 300 K and 420 K, respectively.

reflectance spectroscopy in single crystals of poly-4Un (n=2-5). PDA chains usually show a strong optical transition due to the ^1B_u exciton around 2 eV which is polarized along the polymer chain axis. In poly-4Un crystals the reflectance peak due to the exciton transition is located at 1.94 eV-1.95 eV at 300 K, but shifts to about 2.30 eV at 420 K, as shown in Fig.IV-3 for n=2-5. This shift causes a drastic color change from gold (or blue in thin films) to red.

For the other poly-4Un's (n=1,6-10), single crystal samples of macroscopic size were hard to be obtained, so that absorption spectra were measured on polycrystalline powders dispersed in KBr pellets. In those spectra, the strong absorbance peaks due to the ^1B_u exciton were also observed at about the same energies as observed in single crystals: The energies of the ^1B_u excitons observed at low (300 K) and high (420 K) temperatures nearly coincide with those in the so-called A(blue)- and B(red)-phases of other thermochromic PDAs [IV-4]. This shows that the thermochromic phase transition (the A-B transition) is a general feature in the family of poly-4Un crystals, which should be associated with common structural change in conjugated polymer backbones of these PDAs.

To determine critical temperatures of the thermochromic phase transitions in poly-4Un series, we adopted the following two methods: The first was to trace the temperature-dependent reflectivity at the energy of the exciton peak in the A-phase (ca.1.94 eV). As seen in Fig.IV-3, the reflectivity at the A-phase exciton peak (1.94 eV) considerably decreases in the B-phase due to the apparent blue-shift of the exciton peak, and hence it serves as a sensitive probe for the A-B transition. The second

method to detect the phase change was the conventional differential scanning calorimetry (DSC). The phase transitions in poly-4Un crystals mostly show up as clear endothermic and exothermic peaks as shown below.

In Fig.IV-4 are shown the temperature-dependence of the reflectivity at the A-phase exciton peak energy (1.94 eV) and the DSC thermograms in poly-4U4 crystals for thermal cycles in which the upper limit of temperature scan is (a) about 433 K and (b) about 515 K. The reflectivity trace shown in Fig.IV-4(a) draws a typical hysteresis loop characteristic of the reversible A-B transition. The critical temperatures for the A-to-B transition in the heating process (T_2) and those for the B-to-A transition in the cooling process (T_1) have been determined taking half points of the reflectivity change as indicated by filled circles in the Fig.IV-4.

Such a reversible feature is clearly seen also in the DSC thermogram. As shown in Fig.IV-4(a), the endothermic and exothermic peaks with an enthalpy change (ΔH=2.5$\pm$ 0.1kcal/mol) are observed in the heating and cooling runs (at the rate of 10 K/min.), respectively, in poly-4U4 crystals. The peak positions in the thermogram well correspond to the transition temperatures, T_2 for the A-to-B and T_1 for the B-to-A transition , determined from the reflectivity change. In other words, we can determine T_1 and T_2 for various poly-4Un crystals by measuring the reflectivity change or the DSC thermogram.

When temperature is increased further beyond ca.500 K, the thermochromic change becomes irreversible, as shown in Fig.IV-4(b). The reflectivity monitored at the energy of the

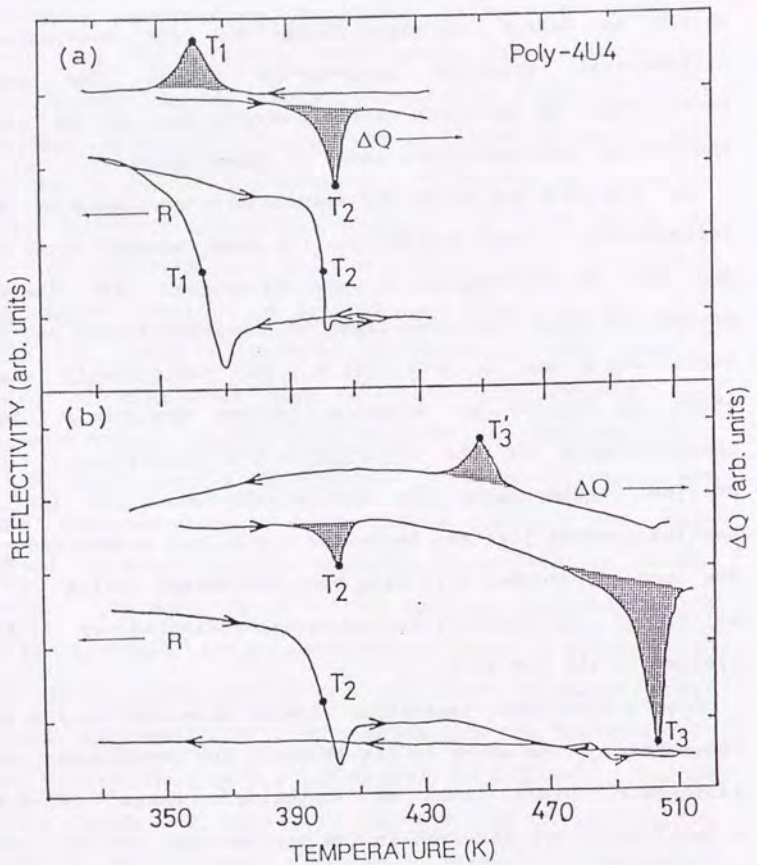

Figure IV-4 : Temperature-dependence of reflectivity in poly-4U4 crystal at 1.94 eV and thermograms by differential scanning calorimetry (DSC). The sample was heated up to 433 K in case (a) and up to 515 K in case (b).

A-phase exciton peak drops at the A-to-B transition temperature T_2, but does not recover any more in the cooling run once temperature is increased beyond 500 K. The DSC curve in the heating run shows a large endothermic peak around T_3=503 K in addition to that at T_2 for the A-to-B transition. The peak at T_3 is clearly attributed to the melting of polymer crystals. In the cooling run the DSC curve shows an exothermal peak at a lower temperature (T'_3) due to the solidification. Such a melt-recrystallized sample remains to be red even below T'_3 or T_1 and its reflectance and Raman spectra rather resemble those in the B-phase (for the detail, see the discussion in sec.IV-3-4).

Qualitatively similar behavior of the reversible and irreversible thermochromic transitions has been observed in all poly-4Un (n=1-10) crystals investigated in this work. In Fig.IV-5 are plotted the transition temperatures, T_1 and T_2, for the reversible thermochromism (A-B transition) in all poly-4Un crystals, together with the melting temperature T_3. Thermochromic hystereses (T_1 and T_2) were determined by the above-mentioned measurements of the reflectivity (or absorbance) change and the DSC thermogram. It is seen in Fig.IV-5 that T_1 and T_2 show an oscillation according to the even-odd parity of n, indicating that the conformation of outer alkyl chain is contributing to the A-B phase transition. Nevertheless, the variation of T_1 and T_2 with n is not so significant, implying more important influence of the inner alkyl chain rather than the outer one.

We can approximately estimate the change in enthalpy upon the A-B transition from the integrated area of the DSC endothermic peak at T_1 or of the exothermic peak at T_2. The

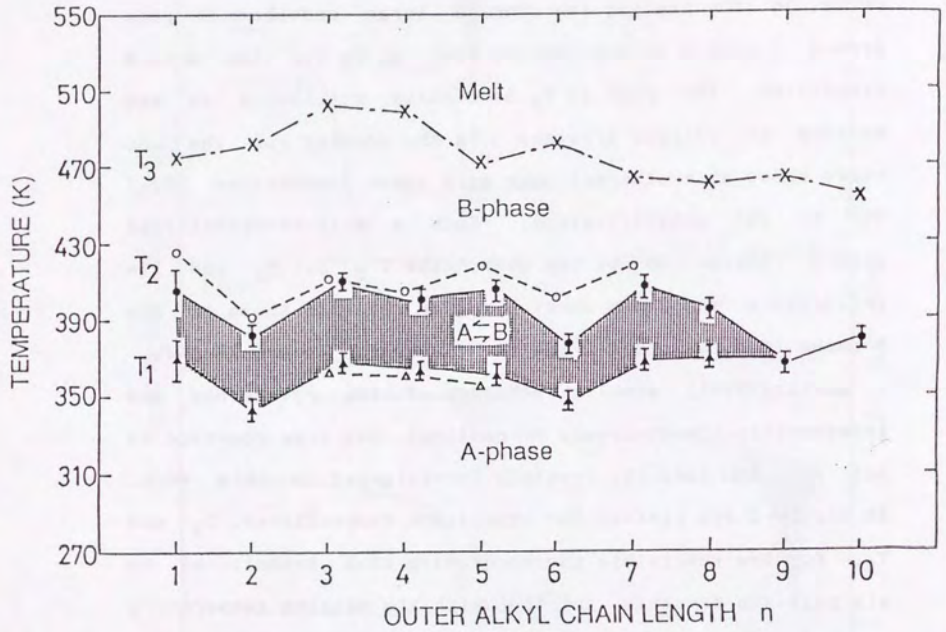

Figure IV-5 : Transition temperatures (T_1, T_2 and T_3) of poly-4Un (n=1-10) obtained by spectroscopic and DSC methods. Values for T_1 and T_2 determined by the spectroscopic method are denoted by filled triangles and filled circles, respectively. Open triangles, open circles, and crosses are for T_1, T_2 and T_3, which were determined by the DSC method.

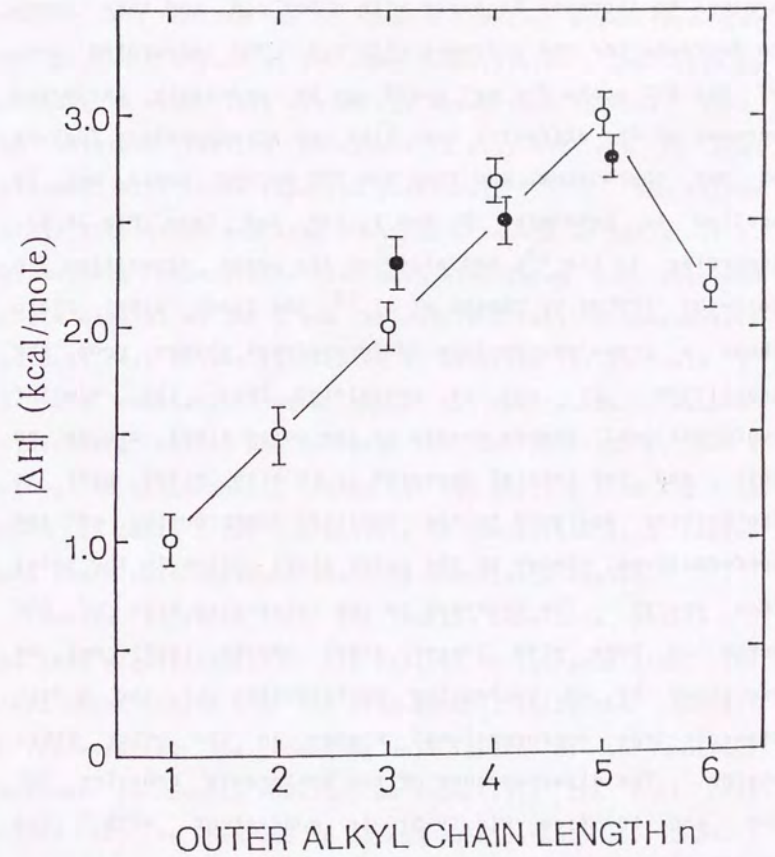

Figure IV-6 : The n-dependence of integrated area of the DSC endothermic peak (open circles) around T_2 and of the exothermic ones (filled circles) around T_1.

results are plotted against the outer alkyl chain length n of the side-group in Fig.IV-6. The enthalpy change ΔH appears to increase linearly with n for $n \leqq 5$, and then tends to decrease for the polymers with $n \geqq 6$. The integrated area of the DSC peaks for $n \geqq 7$ could not be precisely estimated because of the diffusive base line and structureless feature of DSC thermogram, and thus the DSC method could not be applied to determine T_1 and T_2 for $n \geqq 8$ (see Fig.IV-5). According to the ^{13}C NMR study on the phase transition in poly-4U2 (ETCD) by Tanaka et al.[13], the inner alkyl chain shows a trans-gauche-like conformational change upon the transition. It may be postulated that the similar conformational change occurs in the outer alkyl groups as well, and the initial increase in ΔH with n(for $n \leqq 5$) is tentatively assigned to the additive contribution of the conformational change in the outer alkyl chains to the total free energy. The decrease in the integrated area of DSC peaks in PDAs with longer alkyl chains ($n \geqq 6$) may be explained by an increasing contribution of the order-disorder-type conformational change in the outer alkyl chains. The disappearance of the hysteresis behavior for n=9 and 10 (see Fig.IV-5) is consistent with this hypothesis.

IV-3-2 Temperature-dependence of lattice constants in poly-4Un crystals

To examine possible correlation between the thermochromic phase change and structures in the polymers, lattice constants and their temperature-dependence have been investigated by measurement of the X-ray powder diffraction.

The lattice parameters in poly-4Un with n=2,3 and 4 were measured not only at room temperature (300 K) but at a specific temperature in between T_1 and T_2 in both the heating and cooling run to compare lattice parameters for the A- and B-phases at the same temperature. The results assuming a monoclinic system are summarized in Table IV-I. The obtained lattice constants in poly-4U2 are in good agreement with those reported previously[IV-14]. The values in the literature are also shown in brackets in Table IV-I. Weissenberg photographs have been also taken for poly-4U3 single crystal at 300 K and the obtained lattice parameters and unit cell volume (indicated by asterisk (*) in Table IV-I) are consistent with those by the powder method. Weissenberg method has revealed that the poly-4U3 at 300 K belongs to orthorhombic system but the angle β (90 deg.) is shown in table I for convenience of comparison with powder data which were obtained assuming monoclinic system.

Looking at Table IV-I, the lattice constants, mainly a and less significantly c, are noticed to increase with the alkyl chain length n of the side-groups, while the constant b representing the repeating unit length of the polymer backbone is nearly constant as expected. The unit cell volume (V) is observed to expand considerably (by 2-3%) upon the A-to-B transition as is evident from the comparison between the data taken at the same temperature in between T_1 and T_2. Furthermore, it is to be noted that the angle β is close to 90 deg. in the B-phase in each crystal, implying possible monoclinic-to-orthorhombic transition upon the A-to-B transition in the polymer crystals with n=2 and 4.

To see the structural change associated with the thermochromic phase transition in more detail, we show

		a/Å	b/Å	c/Å	β/deg.	V/Å^3	ΔV/V(%)
	A Phase 300 K	18.35(8) [18.13]	4.90(5) [4.89]	10.76(5) [10.81]	95.3(5) [94]	963 [956]	
n=2	A Phase 368 K	18.60(9)	4.91(6)	10.83(6)	94.2(6)	986	2.4
	B Phase 368 K	18.91(9) [18.9]	4.90(6) [4.83]	10.90(6) [10.89]	90.4(6) [91]	1010 [994]	
	A Phase 300 K	*40.39(11) *40.42(5)	*4.81(6) *4.79(2)	*10.83(8) *10.83(3)	*90.2(5) *90	*2100 *2100	
n=3	A Phase 390 K	40.90(13)	4.82(7)	10.97(9)	90.2(7)	2160	2.8
	B Phase 390 K	41.53(13)	4.83(7)	11.09(9)	90.1(7)	2220	
	A Phase 300 K	44.35(12)	4.85(6)	11.40(8)	96.5(6)	2440	
n=4	A Phase 383 K	45.05(14)	4.86(8)	11.79(10)	95.5(8)	2570	3.1
	B Phase 383 K	45.65(14)	4.86(8)	11.93(10)	91.0(8)	2650	

Table IV-I :Lattice constants determined by measurements of powder diffraction patterns assuming monoclinic system, and Weissenberg photographs (indicated by *). Weissenberg method has shown that the poly-4U3 at 300 K belongs to orthorhombic system. The values in brackets are quoted from ref.IV-14. Δ V denotes the difference between the volume of unit cell in the A- and B-phases measured at the same temperatures.

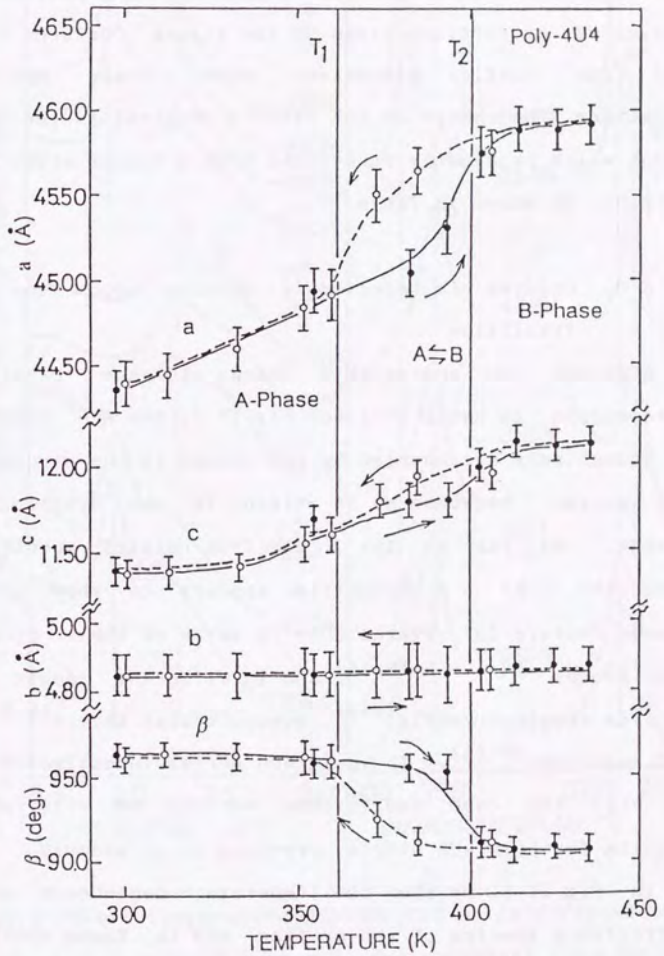

Figure IV-7 : Temperature-dependence of lattice constants of poly-4U4 (a, b, c and β) obtained by the X-ray powder diffraction method. Filled and open circles denote heating and cooling processes, respectively.

temperature-dependence of lattice parameters in poly-4U4 crystals in Fig.IV-7. The phase transition temperatures, T_1 and T_2, determined by the thermochromic behavior are indicated by vertical lines in the figure. Between T_1 and T_2, the lattice parameters show clear hysteresis behaviors. The change of the lattice constant is the largest for a which is closely correlated with n (outer alkyl chain length), as shown in Table IV-I.

IV-3-3. Changes in electronic spectra upon the A-B transition

Although no appreciable change in the b-axis is discernible in Table IV-I nor Fig.IV-7, the A-B transition is undoubtedly accompanied by the change in the structure of the polymer backbone as is evident in the drastic color change. As far as the π-electron-related spectra are concerned, the A-B transition appears to show quite a common feature for several PDAs in spite of their different side-groups [IV-1 - 5,15,16] and in different sample forms such as single crystals[IV-2], monomolecular layers[IV-3,4,15] and solutions[IV-16]. The poly-4Un series investigated here is also the case, and in this section we will present results for poly-4U3 single crystals as an example.

In Fig.IV-8, we show the temperature-dependence of (a) reflectance spectra of the exciton and (b) Raman spectra of the polymer backbone vibrations. The exciton reflectance spectrum shown in Fig.IV-8(a) is polarized along the polymer axis (b-axis) and is composed of the main 0-0 band (denoted as A or B) and its vibronic sidebands (A' or B') due to the coupling with the bond stretching modes. Such vibration

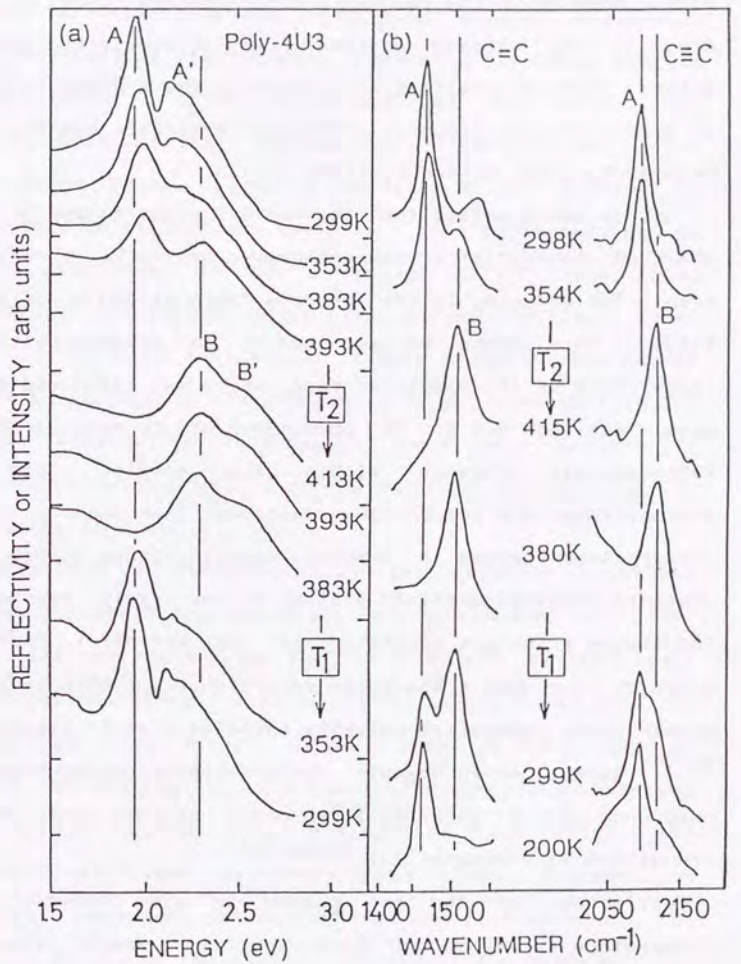

Figure IV-8 : Temperature-dependences of (a)reflectance and (b)Raman spectra of poly-4U3 single crystal for the light polarized parallel to the b-axis (direction of polymer backbones).

modes show up in the resonance Raman spectra (see Fig.IV-8(b)). As already noticed, the reflectivity maximum shifts from the position at 1.94 eV in the A-phase to that at 2.30 eV in the B-phase, showing a hysteresis behavior in between T_2 (=407 K) and T_1 (=365 K).

It is worth noting that the two 0-0 peaks (A and B) are observed to coexist at temperatures close to T_1 or T_2, as seen, for example, in the spectrum taken at 393 K (Fig.IV-8(a)). This cannot be explained by an inhomogeneity of temperature on the sample surface, which was estimated to be much less than 0.5 K. The phenomenon may be related to an inhomogeneity present within the sample, such as dislocations and polymer imperfections. That such a local perturbation causes a semi-macroscopic phase-change is characteristic of quasi-1D systems having nearly degenerate two states which are separated with some potential barrier. Examples for such a two-phase coexistence are also seen in charge-doped conducting polymers associated with bipolarons [IV-17] as well as in organic donor-acceptor charge-transfer compounds which show the first-order neutral-ionic phase transition (see chapter II) [IV-18,19].

Coexistence of the two phases is also observed in temperature-variation of Raman spectra. Raman lines at 1460 cm^{-1} and 2090 cm^{-1} at room temperature shown in Fig.IV-8(b) have been assigned to the stretching vibrations of the double bond and triple bond in the A-phase polymer backbone, respectively. These Raman lines shift to the higher-frequency positions at 1505 cm^{-1} and 2115 cm^{-1} upon the A-to-B transition, respectively, as shown in Fig.IV-8(b). Quantitatively similar changes in Raman spectra at the A-B transition are commonly observed in other PDAs [IV-7,20,21];

not only in other poly-4Un crystals but also in PDAs having different kinds of side-groups. Examining the Raman profile in more detail, it may be noticed that the Raman lines characteristic of the B-phase still survive at lower temperatures below T_1, where the trace of the B-phase is hardly seen in reflectance spectra. This difference can be simply attributed to the resonance effect in Raman scattering: The photon energy (2.41 eV) of incident laser light in the Raman measurement is more close to the energy of the ^1B_u exciton in the B-phase (2.30 eV) than that in the A-phase (1.94 eV). As a result, the B-phase feature is much more pronounced when observed in Raman spectra than in reflectance spectra.

In Fig.IV-9 is shown temperature-dependence of polarized fluorescence spectra measured on the (100) surface of poly-4U3 single crystals. The 514.5nm (2.41 eV) Ar-ion laser line polarized along the polymer axis (b-axis) was used as an exciting light source. In the A-phase at 299 K and at 350 K in the heating run, the hot luminescence was observed just below the exciting energy (2.41 eV) which was overlapped with the resonance Raman lines. However, no prominent emission was observed at energies around the energy (1.94 eV) of the singlet exciton in the A-phase.

Upon the A-to-B transition the emission yield was observed to be remarkably enhanced. In addition to the overlapping sharp Raman lines, broad fluorescence spectra (shaded in the figure) with two peaks around 2.21 eV and 2.05 eV were observed in the B-phase. This fluorescence band is strongly polarized along the polymer chain axis as shown in Fig.IV-9. The energy separation between the two

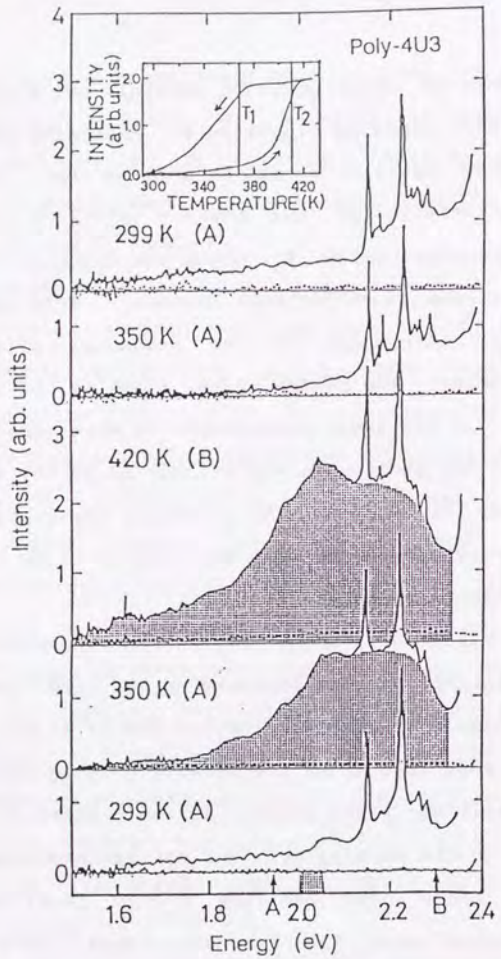

Figure IV-9 : Fluorescence spectra of poly-4U3 at various temperatures polarized parallel (solid line) and perpendicular (dotted line) to the b-axis (direction of polymer backbones). The notations (A) and (B) indicate that the sample is in the A- and B-phase, respectively. Arrows on the abscissa show the energies of the exciton peaks in the A- and B-phases. The inset shows the temperature-dependence of fluorescence intensity integrated over 2.00-2.05 eV (hatched region of the abscissa).

broad peaks (ca. 0.16 eV or 1300 cm^{-1}) well corresponds to that between the 0-0 and 0-1 maxima in the reflectance or absorption spectrum (denoted as B and B' in Fig.IV-8(a)).

From these features as well as their polarization characteristics, the two broad peaks in the fluorescence spectrum observed in the B-phase may be assigned to the Stokes-shifted emission band and its vibronic sideband due to the exciton recombination. However, we have observed that the fluorescence intensity is rather sensitive to the sample quality or to the species of the side-group. Therefore, some impurities or more likely the polymer imperfections may play a role of emission centers where a photo-generated free exciton is trapped and then subject to the lattice relaxation.

In the inset of Fig.IV-9, the temperature-variation of emission intensity integrated over 2.00-2.05 eV is plotted, which again shows a clear hysteresis behavior. The behavior is reproducibly observed for repeated thermal cycles, as far as the temperature is decreased sufficiently below T_1 (e.g. down to room temperature) and is not raised beyond T_3. This indicates that fluorescence observed in the B-phase is not due to a permanent degradation nor to an interruption of the polymer backbones. The fluorescence process is generally in competition with non-radiative decay of the excitons. In the PDA chains with the A-type backbone structure, the non-radiative process seems to overwhelm the radiative process, which is also the case even in dilute PDA solutions with the blue-form (A-type) [IV-22]. Incidentally, a diffuse tail of the fluorescence intensity curve below T_1 in the A-phase may be attributed to the residue of the fluorescent B-type chains.

IV-3-4. Role of hydrogen bonds in side-groups in thermochromic phase transitions

Most of reversibly thermochromic PDAs, including the present poly-4Un series, possess the urethane groups in side-groups as a common structural unit, which are mutually linked to each other by hydrogen bonds running parallel to the polymer backbones as shown in Fig.IV-1. It was argued that the strong hydrogen bonding plays an essential role in maintaining the planarity of the polymer backbone and also that interruption of hydrogen bonds is crucial for the conformational change in dichromatic PDA solutions[IV-6,16,21,22]. Here we present experimental investigation on the correlation between the thermochromic phase changes and strength of hydrogen bonding. Such a study has been made before by Rubner et al. [IV-12] on poly-4U2 (ETCD) and we tried to extend the study to the family of poly-4Un by the simultaneous measurements of infrared (IR), Raman, visible reflectance (or absorption) spectra and DSC thermograms.

To pursue the strength of hydrogen bond between the carbonyl- and amino-groups, IR absorption due to N-H stretching modes around 3300 cm^{-1} can be utilized as a microscopic probe [IV-23]. Fig.IV-10 shows the thermal changes in some key optical spectra in poly-4U5 crystals; (a) reflectance spectra of the exciton, (b) Raman spectra of the double bond stretching mode in the polymer backbone, and (c) the IR absorption spectra of the N-H stretching mode in the side-groups. These features bear information on (a) π-electronic states, (b) the backbone structure, and (c) the

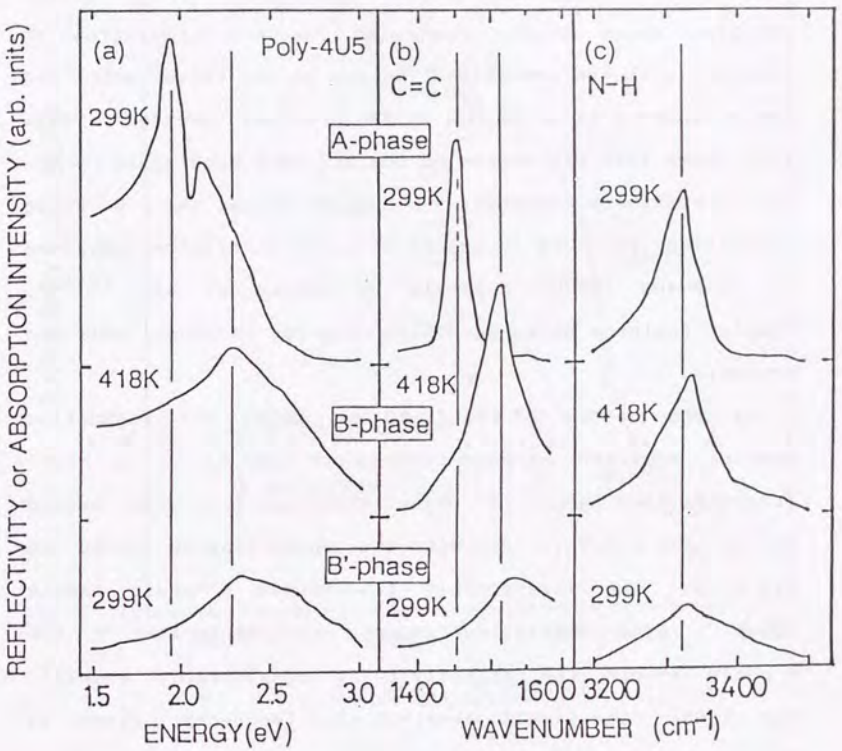

Figure IV-10: (a) Reflectance, (b) Raman and (c) IR absorption spectra of poly-4U5 in the A(top)-, B(middle)- and B'(bottom)-phases. Raman line and IR absorption bands correspond to the C=C and N-H stretching modes, respectively.

strength of hydrogen bonding between the side-groups, respectively. One may notice that the IR absorption spectrum shows little change on the A-B transition in contrast with the remarkable changes in the reflectance and Raman spectra as described in the previous sections. This fact shows that the degree of the hydrogen bonding in poly-4U5 crystals is essentially unchanged during the A-B phase transition, which is in accord with the conclusion obtained on poly-4U2 (ETCD) crystals by Rubner et al. [IV-12]. Similar features have been also observed in other poly-4Un crystals.

At the bottom of Fig.IV-10 are shown the respective spectra measured at room temperature (299 K) on a melt-recrystallized sample (B'-phase) which has been once heated up to 525 K (>T_3), (see also the phase-diagram shown in Fig.IV-5). The irreversibly transformed B'-phase sample shows a rather similar reflectance spectrum to that in the B-phase though the reflectivity is considerably reduced. The Raman line is also observed at a frequency close to that in the B-phase, but shows an extremely blurred profile. Judging from these features, the conformation in the polymer backbone in the B'-phase resembles that in the B-phase, but significantly affected by disorder or interruption of conjugation. It well corresponds to the previously reported results on melt-crystallized ETCD derived from measurements of ^{13}C NMR, X-ray diffraction and electron microscopy[IV-24]. The IR band shown in the bottom of Fig.IV-10(c) shows a broadened feature and the integrated intensity is reduced to about a half, although its peak frequency is almost unchanged.

Temperature-variation of the IR band intensity, or

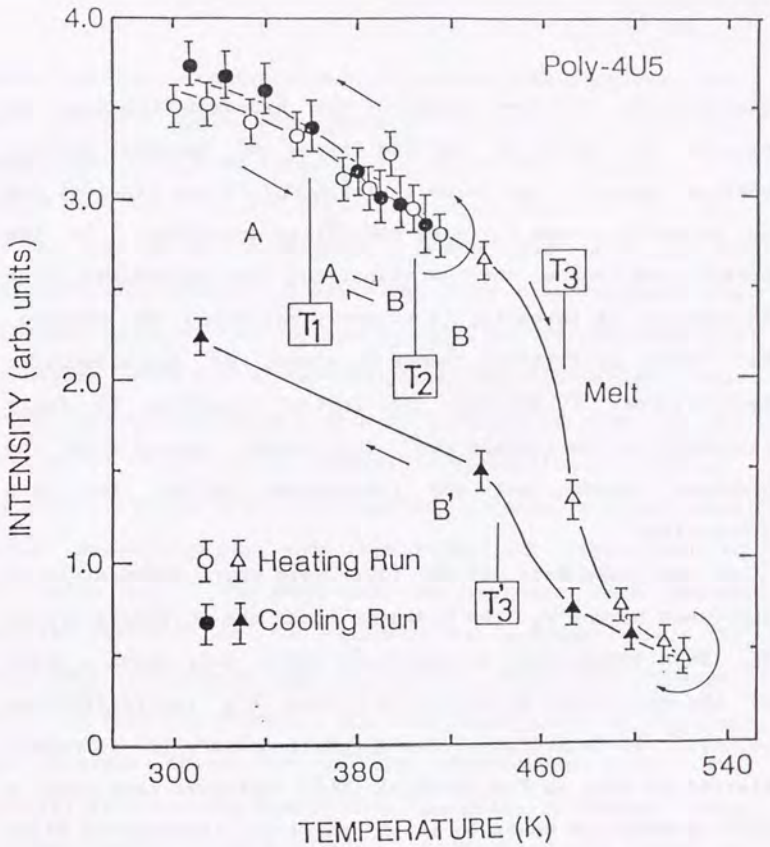

Figure IV-11: Temperature-dependence of IR absorption intensity for the N-H stretching mode in poly-4U5. Open and filled circles represent the results for the process of heating up to 415 K (<T_3) and subsequent cooling, while open and filled triangles for a thermal cycle of heating up to 525 K (>T_3), and cooling.

equivalently of the degree of the hydrogen bonding, is plotted in Fig.IV-11 for two types of thermal cycles; heating above T_2 but below T_3 (open and filled circles) and up to 525 K beyond T_3 (open and filled triangles). In the former run where the A-B transition is reversible, the integrated IR intensity is slightly decreased on heating, but shows no distinct change at either of characteristic temperatures, T_1 and T_2. The initial intensity is fully recovered in the cooling run. This result implies that the hydrogen bonds are not interrupted during the A-B transition.

On the other hand, in the later case where temperature is increased beyond T_3, the hydrogen bonds are collapsed around T_3. When temperature is decreased again, only about a half of the absorbance is recovered around T'_3 (solidification point). At this stage, the spectral feature is extremely blurred as seen in Fig.IV-10(c). This indicates that about a half of hydrogen bonds in the B'-phase are interrupted after the melt-recrystallized process and that the bonding sequence is subject to strong disorder. Together with the conclusions derived from the reflectance and Raman spectra, it may be argued that the disorders in the hydrogen bonding favor for stabilizing the B-type chain conformation. This is consistent with the previous study[IV-6] on poly-crystalline poly-4U2 (ETCD) films of ca. 1000 Å thickness reporting that collapse of about a half of hydrogen bonds around T_2 ($<T_3$) causes the irreversible A-to-B transition[IV-25].

IV-4 CONCLUSION

Universality of the reversible thermochromic (A-B)

transition has been confirmed in poly-4Un (n=1-10) crystals, and the electronic and structural changes during this transition have been investigated by various methods. It turned out that the A-B transition is accompanied not only by the change in the backbone structure but also by the conformational changes of inner and outer alkyl chains. The critical temperatures, T_1 and T_2, for the first-order A-B transition show little dependence on the outer alkyl chain length (n) indicating a much more influential role of the inner alkyl chains in the reversible transition. However, the order-disorder-type conformational change in outer alkyl chains appears to play some role in the A-B transition in PDAs with $n \geq 6$. The existence of hydrogen bond chains running parallel to the backbones is necessary for the reversible A-B transition to occur. When the hydrogen bonds in poly-4Un crystals are once interrupted by heating the crystals above the melting temperature (T_3), the crystals irreversibly change into the phase (B'-phase) with a lower degree of the π-electron conjugation than those in the A- and B-phases.

REFERENCES OF CHAPTER IV

IV-1) Polydiacetylenes, NATO ASI Series E, vol 102, edited by D.Bloor and R.R.Chance (Nijhoff, Dordrecht 1985).

IV-2) R.R.Chance, R.H.Baughman, H.Muller and C.J.Eckhardt, J. Chem. Phys. 67, 3616 (1977).

IV-3) B.Tieke, G.Lieser and G.Wegner, J. Polym. Sci. Polym. Chem. Ed.17, 1631 (1979).

IV-4) T.Kanetake, Y.Tokura and T.Koda, Solid State Commun. 56, 803 (1985).

IV-5) Y.Tokura, Y.Oowaki, T.Koda and R.H.Baughman, Chem. Phys. 88, 437 (1984).

IV-6) Y.Tokura, T.Kanetake, K.Ishikawa and T.Koda, Synth. Met. 18, 407 (1987).

IV-7) K.Ishikawa, K.Fukagai, T.Kanetake, T.Koda, Y.Tokura and S.Koshihara, Synth. Met. 28, D605 (1989).

IV-8) C.Sauteret, J.-P. Hermann, R.Frey, F.Pradere, J.Ducuing, R.H.Baughman and R.R.Chance, Phys. Rev. Lett. 36, 956 (1976).

IV-9) G.M.Carter, J. Opt. Soc. Am.B, 4, 1018 (1987).

IV-10)T.Kanetake, T.Hasegawa, K.Ishikawa, T.Koda, K.Takeda, M.Hasegawa, K.Kubodera and H.Kobayashi, Appl. Phys. Lett. 54, 2287 (1989).

IV-11)H.Tanaka, M.Thakur, M.A.Gamez and A.E.Tonelli, Macromolecules 20, 3094 (1987).

IV-12)M.F.Rubner, D.J.Sandman and C.Velazquez, Macromolecules, 20, 1296 (1987).

IV-13)H.Tanaka, M.A.Gomez, A.E.Tonelli and M.Thakur, Macromolecules 22, 1208 (1989).

IV-14)M.J.Downey, G.P.Hamill, M.Rubner, D.J.Sandman and C.S.Velazquez, Makromol. Chem. 189, 1199 (1988).

IV-15)G.Lieser, B.Tieke and G.Wegner, Thin Solid Films 68, 77 (1980).

IV-16)G.N.Patel, R.R.Chance and J.D.Witt, J. Chem. Phys, 70, 4387 (1979).

IV-17)T.C.Chung, J.H.Kaufman, A.J.Heeger and F.Wudl, Phys. Rev.B 30, 702 (1984).

IV-18)J.B.Torrance, A.Girlando, J.J.Mayerle, J.I.Crowley, V.Y.Lee and P.Batail, Phys. Rev. Letters, 47, 1747 (1981).

IV-19)Y.Tokura, T.Koda, G.Saito and T.Mitani, J. Phys. Soc. Jpn. 53, 4445 (1984).

IV-20)G.J.Exarhos, W.M.Risen Jr. and R.H.Baughman, J. Am. Chem. Soc. 98, 481 (1976).

IV-21)M.L.Shand, R.R.Chance, M.LePostollec and M.Schott, Phys. Rev. B 25, 4431 (1982).

IV-22)T.Kanetake, Y.Tokura, T.Koda, T.Kotaka and H.Ohnuma, J. Phys. Soc. Jpn. 54, 4014 (1985).

IV-23)D.J.Skrovanek, S.E.Howe, P.C.Painter and M.M.Coleman, Macromolecules 18, 1676 (1985).
D.J.Skrovanek, P.C.Painter and M.M.Coleman, Macromolecules 19, 699 (1986).

IV-24)H.Tanaka, M.A.Gomez, A.E.Tonelli, A.J.Lovinger, D.D.Davis and M.Thakur, Macromolecules 22,2427 (1989).

IV-25)T.Hasegawa and K.Ishikawa (private communication).

CHAPTER V

Bi-directional Photo-switching between the Two Phases in Single Crystals of Polydiacetylenes

V-1 Introduction

In the previous chapter, the thermally-induced chromatic transition between the two spectroscopically distinct phases, A(blue) and B(red) phases, in polydiacetylenes (PDAs) has been discussed. It was shown that the thermochromic transition in an alkyl-urethane substituted PDA [$\{R'C-C\equiv C-CR\}_x$:R=R'=$(CH_2)_4OCONH(CH_2)_{n-1}CH_3$] (n=1-10) (poly-4Un) is the first order one with large hysteresis width exceeding 60deg.. Therefore, poly-4Un is appropriate system for the study of the reversible phase transition by "photo-excitation" as discussed in chapter I. In this chapter, we demonstrate, for the first time, that this novel phase transition occurs in poly-4U3 single crystals.

In previous works, photo-induced irreversible A-to-B color change has been reported in some PDAs[V-1 - 5]. In those cases, excitation intensity was more than one hundred times stronger than the present study. It was confirmed that such a strong photo-irradiation on PDAs at low temperature induces irreversible disorder in side groups[V-5]. As mentioned in the previous chapter, disorders in side groups (e.g. interruption of hydrogen bond) favor the B-type chain conformation. Therefore, we speculate that strong photo-excitation cause permanent change in side groups and results in the irreversible A-to-B transition. In the present study, the intensity of the excitation light was

carefully controlled and kept as weak as possible not to induce the disorder in side groups, i.e. not to trigger the irreversible A-to-B transition.

V-2 Experimental

Single crystals of poly-4U3 have been prepared by the same method as mentioned in chapter IV. Reflectance spectra before and after photo-excitation have been obtained by about the same experimental apparatus shown in chapter II. Photo-induced changes in Raman spectra have been observed by polychromator coupled with image intensified diode array. Samples have been kept in vacuum during experiment to avoid possible reaction with oxygen.

V-3 Results and Discussion

We have carried out measurements on photo-induced effect in the temperature region where the A and B phases can coexist. Fig.V-1 shows the typical hysteresis loop of A-B transition observed by the measurement of the temperature dependence of reflectivity at 1.95 eV. The reflectivity at 1.95 eV is a good probe for the A-B transition, because the reflectance maximum due to the ^1B_u exciton at ca. 1.95 eV in the A phase shifts to around 2.4 eV in the B phase as mentioned in the previous chapter. Sample has been heated up and cooled down in the order indicated by arrows in the figure. Schematic diagrams of total energy are also shown in Fig.V-1. In the temperature region above "point 2" (below "point 4") the B (A) phase is stabler than the A (B) phase. Between point 4 and 2, the energy levels of both phases will be nearly degenerate.

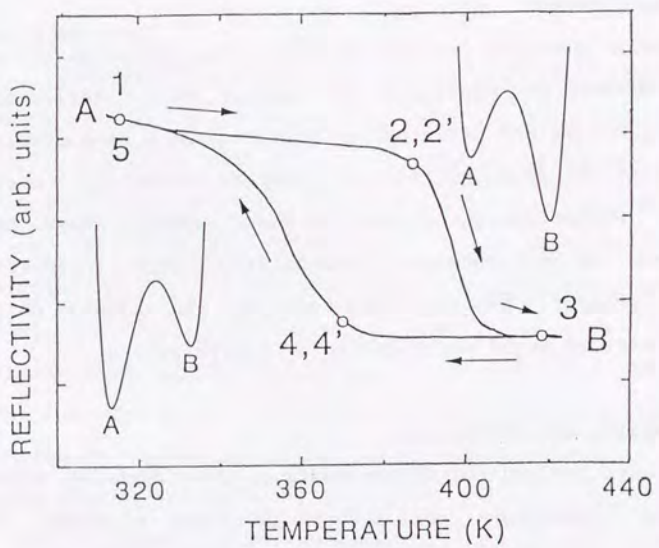

Figure V-1 : Temperature dependence of reflectivity in poly-4U3 crystal at 1.95 eV, and schematic diagrams of total free energy. The temperature points at which the reflectance and Raman spectra were observed, are denoted by open-circles and numbered in the order of heating and cooling process. The numbers 2' and 4' indicate the points where photo-excitation was made.

Spectra of the imaginary part of dielectric constant (ε_2) were obtained by Kramers-Kronig analysis of reflectance spectra at temperatures which corresponds to the numbered point on hysteresis loop. The results are shown in Fig.V-2. To confirm the backbone structure change, we have also measured the Raman spectra in the wavenumber region correspond to C=C stretching mode as shown in Fig.V-2. Raman band located around 1450 cm^{-1} in the A phase shifts to 1500 cm^{-1} in the B phase. The sample at "point 2" and "point 4" was excited by a single pulse from excimer pumped dye-laser (20 ns width) and spectra after photo-excitation (indicated by 2' and 4' in the figure) are shown by dashed-lines. Photon energies of dye-laser were 2.81, and 3.18 eV for points 2, and 4, respectively. (Dependences of efficiencies of A-B transition on the excitation photon energy and intensity is discussed in the following section.) Comparing spectra before and after photo-excitation at the point 2, changes of the both ε_2 and Raman spectra clearly show that more than 85% of the A phase is converted into B phase and about 50% of the B phase into the A phase at point 4.

The excitation intensity dependence of converted fractions by photo-excitation in the both directions (A-to-B and B-to-A) are shown in Fig.V-3. The exciting photon density in the both cases have been obtained assuming the total photon flux of pump light is absorbed uniformly within the attenuation depth of ca. 1μm which is estimated from the absorption spectra in thin film form. The converted fractions were estimated from changes in the integrated intensity of Raman peaks attributed to C=C stretching mode. In the both directions, the efficiencies of photo-induced

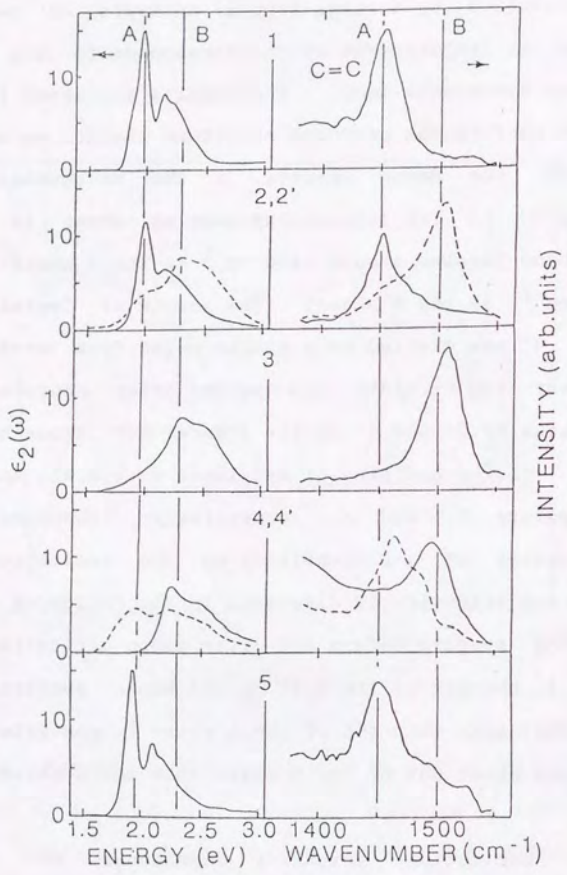

Figure V-2 : Spectra of imaginary part of dielectric constant (ε_2) (left) and Raman spectra due to C=C stretching mode (right) at various temperatures which are shown by open circles on the hysteresis loop in Fig.V-1. ε_2 was calculated from reflectance spectrum using Kramers-Kronig transformation. Dashed lines at temperature points 2' and 4' show the spectra after photo-excitation by pulsed dye-laser.

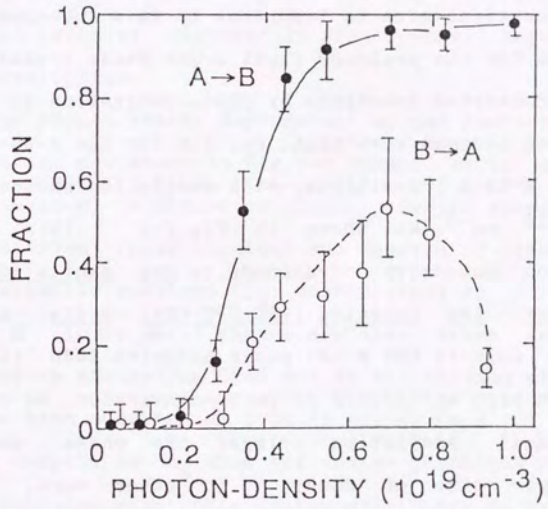

Figure V-3 : Excitation photon density dependence of photo-induced transition efficiencies in the A-to-B (closed circles) and B-to-A (open circles) directions. Excitation photon energies are 2.81, and 3.18 eV for the A-to-B, and B-to-A conversion, respectively.

changes seem nonlinearly depend on the excitation intensity, showing threshold at ca.3×10^{18} cm^{-3}. This suggests that cooperative interaction between photo-excited species plays some role in promoting the phase changes in a macroscopic scale . In particular, formation of the domain with a critical size is important in this phenomenon like the cases for the ordinary first order phase transitions.

The converted fractions by photo-excitation in the both directions becomes very high, ca. 1.0 for the A-to-B and 0.5 for the B-to-A transitions, with excitation photon density of 7×10^{18} cm^{-3} as shown in Fig.V-3. This value of excitation intensity corresponds to one excitation photon for every 140 repeated [$\{RC-C\equiv C-CR\}$] units, since one repeated unit in the A (B) phase occupies 1080 (1110) $\mathring{A}^3$. From such high efficiency of photo-conversion, we can deduce that local excitation trigger the phase change in macroscopic size of domain. In other word, it is evidenced that bi-directional (A to B and B to A) photo-induced phase transition occurs in poly-4U3 single crystal as expected.

The estimated efficiency of the A-to-B transition becomes very high (ca. 100%) and saturates around 5×10^{18} cm^{-3}. In the case of B-to-A transition, the converted fraction clearly decreases as the excitation intensity exceeds 9×10^{18} cm^{-3}. Furthermore, when the crystal in B phase is excited with photon-density exceeding 1×10^{19} cm^{-3}, some irreversible change take place; the over-irradiated crystals show the B-phase like Raman and reflectance spectra even when they are cooled down to the liquid nitrogen temperature (77K). (However, the photo-induced change is observed to be

recoverable by thermal cycle as far as the excitation photon density is less than 7×10^{18} cm^{-1}.) From the previously reported results[V-5] which are mentioned in the beginning of this chapter, we tentatively assign the decrease in B to A converted fraction of over-irradiated crystal to the photo-induced transition from the B phase without hydrogen bond interruption (without disorder in side groups) into that with the interruption.

Excitation photon energy dependences of the photo-induced A-B conversion are shown in Fig.V-4 (upper part: A-to-B, lower part:B-to-A) by closed circles. Action spectra of photoconductiviies (open circles) and spectra of imaginary part of dielectric constant (ε_2: dashed-line) in A (upper part) and B (lower part) phases are also drawn in this figure. Strong absorption band due to the exciton with ^1B_u symmetry has been observed at 1.98 (2.32) eV in A (B) phase. The arrows denoted as ^1A_g show the energy positions of the optically inhibited electronic states attributed to excitons with ^1A_g symmetry[V-6]. These energy positions of ^1A_g exciton in A and B phases were determined by the electric-field modulation spectroscopy.

It is notable that efficiency of photo-conversion and photo-current keep low values in the energy region of strong absorption band due to ^1B_u exciton and both increase parallel at the energy of ^1A_g exciton. This result clearly shows that excitation photon energy larger than ^1A_g exciton is necessary for the carrier generation and the promotion of photo-induced phase transition (i.e. photo-generation of domain-wall between A and B phases). The parallel behavior of photo-current and photo-converted fraction suggests the close correlation between photo-carrier and photo-injected

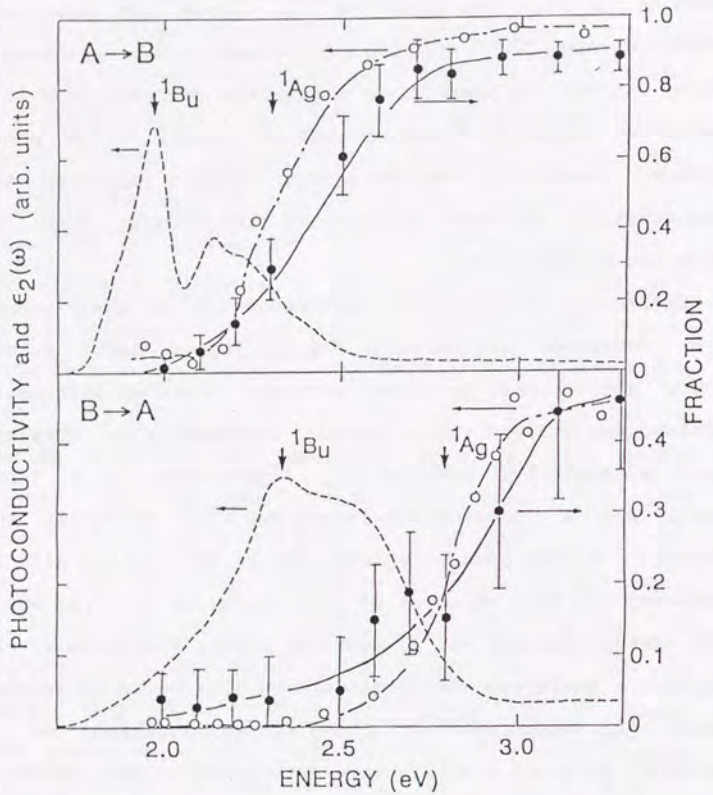

Figure V-4 : Excitation photon energy dependence of photo-converted fractions (closed circles) for the A-to-B (upper part) and B-to-A (lower part) directions. Absorbed excitation photon density was always kept constant value, 6.5×10^{18} cm^{-3}. Open circles show the action spectra of photoconductivity. Spectra of imaginary part of dielectric constants (ε_2) in the A (upper) and B (lower) phase are shown by broken lines. Energy positions of ^1A_g exciton in both A and B phases were determined by the electric field modulation spectroscopy[V-6].

domain-wall between A and B phases. A possible explanation of this correlation is bipolaron (or polaron pair) model. The photo-generated excitonic state may relax to bipolaron state and decompose into a distant polaron pair. This polaron pair is expected to behave as a domain-wall pair and carry charge like the case of charge-doped conducting polymers[V-7]. Of course, this model is speculation and dynamical study is necessary to confirm the relation between photo-carrier and domain wall from the view point of the microscopic mechanism of relaxation process in PDAs.

V-4 Conclusion

In this chapter, we have reported observation of the reversibly photo-induced novel phase transition in polydiacetylene single crystal by thermally controlling the energy level difference between the two (A and B) phases. From a view point of photochromism, the present photo-induced phase transition is quite efficient: The excitation intensity, which is necessary for converting the whole (A-to-B) and 50% (B-to-A) of the crystal, is estimated to be as low as one absorbed photon per 140 repeated {CR-C≡C-CR} units. Threshold behavior in the excitation intensity dependence of converted fraction suggest the existence of critical size of converted domain for driving photo-induced phase transition in a macroscopic scale. Excitation photon energy dependence of converted fraction shows close correlation between generation of photo-carriers and A-B domain walls.

For the detailed study of the microscopic mechanism of A-B transition, the temporal behavior of A-B domain-wall is

necessary as mentioned before. However, time-resolved reflectance and Raman spectra measured by pump-probe technique, cannot be reported in this thesis due to the difficulty in getting sufficient amount of single crystal with high quality. Time-resolved study is now in progress and we expect that it will make clear the dynamics and mechanism of photo-induced A-B transition.

REFERENCES OF CHAPTER V

V-1) Y.Tokura, T.Kanetake, K.Ishikawa and T.Koda, Synth. Metals, 18, 407, (1987).

V-2) Y.Tokura, K.Ishikawa, T.Kanetake and T.Koda, Phys. Rev.B, 36, 2913, (1987).

V-3) K.Ishikawa, K.Fukagai, T.Kanetake, T.Koda, Y.Tokura and S.Koshihara, Synth. Metals, 28, D605, (1989).

V-4) K.Fukagai, K.Ishikawa, T.Kanetake, T.Koda, S.Koshihara and Y.Tokura, Jap. J. Appl. Phys. 29, L977, (1990).

V-5) T.Kanetake, Ph. D. Thesis, The University of Tokyo, (1989).

V-6) T.Hasegawa, K.Ishikawa, T.Kanetake, T.Koda, K.Takeda, H.Kobayashi and K.Kubodera, Chem. Phys. Lett., 171, 239, (1990).

V-7) T.C.Chung, J.H.Kaufman, A.J.Heeger and F.Wudl, Phys. Rev.B, 30, 702, (1984).

CHAPTER VI

Summary

In this thesis, we have studied on the novel photo-induced effect in three kinds of organic crystals; (1) one-dimensional charge-transfer compound, TTF-CA, which shows neutral-ionic transition, (2) one-dimensional radical salt, K-TCNQ, in which the spin-Peierls like transition occurs, (3) one-dimensional conjugated polymer, PDA, substituted with alkyl-urethane side groups which is well known for the thermochromic (A-B) transition. In all systems, it has been confirmed that the photo-injected local excitation can generate a mesoscopic size of domain with different order-parameter or cause the phase transition via some cooperative interaction in crystals.

Obtained results are as follows:

(1) In TTF-CA, large neutral domain is injected into the ionic stack by photo-excitation and one absorbed photon on the surface of TTF-CA single crystal changes 160 ionic DA pair into quasi-neutral state.

(2) Photo-excitation of K-TCNQ in the low temperature phase with dimerized stack, change the amplitude of BOW (dimerization). The observed phase change (not permanent but transient) may be viewed as inverse spin-Peierls transition. In this case, one absorbed photon into dimerized stack generates the homogeneously stacked domain composed of 40 $TCNQ^-$ molecules.

(3) Reversibly photo-induced A-B transition was discovered in poly-4U3 single crystals. The photo-excitation with density of only one excitation photon per 140 repeated units converts more than 50% of the crystal into the other phase.

(4) In all systems, close correlation between photo-generated domain-walls and photo-carriers have been confirmed.

In the present study, fast relaxation process from local excitation into domain-wall cannot be studied for the limit of resolution-time of the experimental apparatus. Study of fast dynamics and its temperature-dependence is very important for the comparison with theoretical works, which is an interesting problem to be tackled in the near future.